CERN-TH.5527/89

Electroweak Radiative Corrections for Z Physics

M. Consoli, W. Hollik, F. Jegerlehner

CERN - Geneva

Contents

To appear in the Proceedings of the Workshop on Z Physics at LEP,
edited by G. Altarelli, R. Kleiss and C. Verzegnassi

CERN-TH.5527/89
September 1989

1 Introduction

The present theory of the electroweak interaction, known as the "Standard Model", is the Glashow-Salam-Weinberg model [1] of leptons, extended via the GIM mechanism [2] to the hadronic sector thus incorporating the idea of Cabibbo mixing [3], and made anomaly free through the introduction of the concept of color [4]. As such it is the most comprehensive description of the electroweak phenomena being theoretically consistent, in agreement with all known experimental tests, and the result of a long historical path culminated in the spectacular discovery [5] of the intermediate vector bosons $W^{\pm}$, Z at the CERN $p\bar{p}$ collider.

The forthcoming experiments with the LEP/SLC e^+e^- accelerators open a new era of precision experiments in the area of electroweak interactions. The detailed investigation of e^+e^- annihilation around the Z resonance should allow the detection of small, calculable deviations from the lowest order predictions for many physical quantities thus providing tests of the theory at the level of quantum corrections. This will confirm the validity of the Standard Model as a fully fledged quantum field theory, in complete analogy to what has been done for QED, or signal the need for some significant modifications.

Loop effects in the Standard Model play, however, an additional important role. Radiative corrections represent an extraordinary "window to new physics" in those situations where the decoupling theorem [6] (i.e. the statement that very heavy particles should not affect the physics at low energies) does not hold automatically, as in the case of spontaneously broken theories. According to quantum field theory the virtual presence of all physical states in the spectrum shows up in higher order calculations. Due to the renormalizability [7] of the Standard Model, particles which up to now have not been directly observed as the Higgs boson, the remnant of the spontaneous symmetry breaking, or the top quark, the missing member of the third fermion generation, will affect the theoretical predictions for the various physical quantities in a calculable way. The same ideas apply, in principle, to all kinds of objects connected with structures beyond the "minimal" standard model (like more Higgs fields, supersymmetric partners, new vector bosons,...). In this case one may also consider modifications of the tree level Lagrangian. The interesting possibility of small zeroth order deviations which mimic or cancel the effect of radiative corrections will not be considered here as it is fully discussed in the "New Physics" section of this report.

Higher order effects related to the presence of the Higgs particle, the top quark, as well as to the self interaction of the gauge fields represent the "genuine" radiative corrections of the electroweak theory. Their typical size in observable quantities is expected to be $\delta_W \leq O(10^{-2})$. Their observation requires therefore that the theoretical uncertainties are of the order of $O(10^{-3})$. In particular the QED corrections, common to any theory which includes the electromagnetic U(1) subgroup, have to be clearly disentangled in the theoretical predictions and in the analysis of the experiments.

The electroweak Standard Model contains, besides fermion masses, quark mixing angles, and the mass of the Higgs scalar, three free parameters in the gauge sector. For a comparison between theory and experiment three independent experimental input

data are required for fixing the SU(2) and U(1) gauge coupling constants g_2, g_1, and the vacuum expectation value v of the Higgs field. It is, however, more practical to deal with parameters such that each of them has a direct relation to a specific experiment and is a well measured quantity. For Z physics at LEP the most natural choice is given by the electromagnetic fine structure constant α (Thomson scattering), the Fermi constant G_μ (muon lifetime), and the mass of the Z boson (Z line shape). The masses of the Higgs boson and the top quark will enter the higher order calculations as additional free parameters unless a direct experimental determination of their values is available.

The calculation of QED corrections also in higher than one-loop order [8-12] and the precise calculation of the Z boson width [13,14] are essential to determine theoretically the Z line shape [15,16] from which M_Z will be measured. The position of the peak maximum and its relation to M_Z turns out to be insensitive to the values of the other parameters [15] which is crucial for M_Z being an independently measurable input parameter (see also the "Z Line Shape" contribution).

In this report we follow the line of the on-shell scheme which treats the masses of the vector bosons M_Z and M_W in a symmetric way: the one-loop amplitudes for 4-fermion processes are expressed in terms of M_Z and M_W (besides α) as the basic quantities defined as the real parts of the pole positions in the Z and W propagators. The decay constant G_μ, measured from the muon lifetime, can then be calculated as a constraint

$$G_\mu = G(\alpha, M_Z, M_W, M_H, m_t)$$

on the value of M_W after specifying the other quantities. In practice this constraint is used to determine the numerical value for M_W entering the amplitudes for $e^+e^- \to f\bar{f}$. This removes the dependence of the measurable quantities around the Z peak (integrated cross sections, total and partial widths, forward-backward asymmetry and τ-polarization) on an explicit W mass measurement.

It is the purpose of this report to provide the building blocks for the calculations of radiative corrections and their implementation in e^+e^- annihilation amplitudes. Moreover, a discussion of the leading terms from light and heavy fermions is presented including $O(\alpha^2)$ contributions, and approximate formulae are given which allow to incorporate the large terms in a simple Born like amplitude ("improved Born approximation"). In section 2 we give a collection of the lowest order relations between the basic parameters, and the differential cross section for $e^+e^- \to f\bar{f}$. Section 3 is a short description of the renormalization in the on-shell scheme, whereas section 4 contains the concrete results for e^+e^- processes, together with the approximate formulae, and the leading higher order effects. In section 5 we discuss briefly the quantity Δr in the relation between G_μ-M_W-M_Z as far as it is of general interest for the purpose of this introduction.

2 Lowest order expressions

In this section we want to provide a set of formulae following from the tree level Lagrangian which allows us to perform calculations of measurable quantities in lowest order. Explicit results are given for the $e^+e^- \to f\bar{f}$ cross section and for the fundamental relation between the vector boson masses, α and G_μ.

2.1 Feynman rules for gauge-field fermion interactions

The gauge invariant Higgs-gauge field interaction leads to mass terms for the vector bosons which are non-diagonal in the basic SU(2) and U(1) fields:

$$\frac{1}{2}\left(\frac{g_2}{2}v\right)^2 (W_1^2 + W_2^2) + \frac{v^2}{4}\left(W_\mu^3, B_\mu\right)\begin{pmatrix} g_2^2 & g_1 g_2 \\ g_1 g_2 & g_2^2 \end{pmatrix}\begin{pmatrix} W_\mu^3 \\ B_\mu \end{pmatrix}. \tag{1}$$

The physical content becomes transparent by performing the transformation from the fields W_μ^a, B_μ (in terms of which the symmetry is manifest) to the "physical" fields

$$W_\mu^\pm = \frac{1}{\sqrt{2}}(W_\mu^1 \pm W_\mu^2) \tag{2}$$

and

$$\begin{aligned} Z_\mu &= +\cos\theta_W W_\mu^3 + \sin\theta_W B_\mu \\ A_\mu &= -\sin\theta_W W_\mu^3 + \cos\theta_W B_\mu \end{aligned} \tag{3}$$

In these fields the mass term (1) is diagonal and the masses are given by

$$\begin{aligned} M_W &= \frac{1}{2} g_2 v \\ M_Z &= \frac{1}{2}\sqrt{g_1^2 + g_2^2}\, v \end{aligned} \tag{4}$$

if the mixing angle in (3) is chosen as

$$\cos\theta_W = \frac{M_W}{M_Z} = \frac{g_2}{\sqrt{g_1^2 + g_2^2}}. \tag{5}$$

Identifying A_μ with the photon field which couples via the electric charge $e = \sqrt{4\pi\alpha}$ to the electron, e can be expressed in terms of the gauge couplings in the following way

$$e = \frac{g_1 g_2}{\sqrt{g_1^2 + g_2^2}} \tag{6}$$

or

$$g_2 = \frac{e}{\sin\theta_W}, \quad g_1 = \frac{e}{\cos\theta_W}. \tag{7}$$

For the important class of charged and neutral current processes between fermions the coupling constants for the vector and axial vector currents can be expressed in terms of

the parameters ϵ, M_W, M_Z as follows:

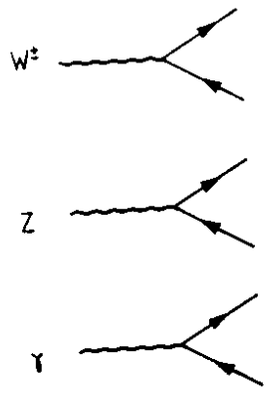

$$\begin{aligned} &= i e \gamma_\mu (1 - \gamma_5) \frac{1}{2\sqrt{2}\sin\theta_W} \\ &= i e \gamma_\mu (v_f - a_f \gamma_5) \\ &= -i e Q_f \gamma_\mu \end{aligned} \tag{8}$$

The neutral current coupling constants in (8) are given by

$$v_f = \frac{I_3^f - 2Q_f \sin^2\theta_W}{2\sin\theta_W\cos\theta_W}, \quad a_f = \frac{I_3^f}{2\sin\theta_W\cos\theta_W} \tag{9}$$

where I_3^f and Q_f denote the third isospin component and the electric charge of a given fermion species f.

Together with the photon propagator (Feynman gauge)

$$-\frac{i g^{\mu\nu}}{k^2} \tag{10}$$

and the W and Z propagators in the unitary gauge ($V = W, Z$)

$$i\frac{-g^{\mu\nu} + k^\mu k^\nu / M_V^2}{k^2 - M_V^2} \tag{11}$$

we have a set of rules allowing the calculation of cross sections and lifetimes for neutral and charged current processes at the tree level.

2.2 Muon lifetime

The Fermi model with an effective coupling constant G_μ gives an expression for the muon lifetime τ_μ from which the value of G_μ is determined. Taking into account the electromagnetic corrections to muon decay in the Fermi model [17]

$$\frac{1}{\tau_\mu} = \frac{G_\mu^2 m_\mu^5}{192\pi^3}\left(1 - \frac{8m_e^2}{m_\mu^2}\right)\left[1 + \frac{\alpha}{2\pi}(1 + \frac{2\alpha}{3\pi}\log\frac{m_\mu}{m_e})(\frac{25}{4} - \pi^2)\right] \tag{12}$$

the very precise measurement of τ_μ yields [1]

$$G_\mu = 1.166389(22) \cdot 10^{-5}\mathrm{GeV}^{-2}\,.$$

Application of the Standard Model in lowest order to the muon lifetime and identification with the Fermi model result (without the QED correction factor) lead to the relation

$$G_\mu = \frac{\pi\alpha}{\sqrt{2}} \cdot \frac{1}{M_W^2 \sin^2\theta_W}\,. \tag{13}$$

By adding the relation, valid for Higgs doublets:

$$\sin^2\theta_W = 1 - \frac{M_W^2}{M_Z^2} \tag{14}$$

we have a correlation between the mass values M_W and M_Z since α and G_μ are known with practically negligible experimental errors. This means that, after M_Z has been specified, also M_W and $\sin^2\theta_W$ are fixed:

$$M_W^2 = \frac{M_Z^2}{2}\left(1 + \sqrt{1 - \frac{4A}{M_Z^2}}\right) \tag{15}$$

$$\sin^2\theta_W = \frac{1}{2}\left(1 - \sqrt{1 - \frac{4A}{M_Z^2}}\right) \tag{16}$$

where

$$A = \frac{\pi\alpha}{\sqrt{2}G_\mu} = (37.2802 \pm 0.0003\,\mathrm{GeV})^2\,. \tag{17}$$

The relations (13 - 16) are in general modified by the inclusion of radiative corrections depending on the details of a chosen renormalization scheme. In the on-shell scheme (14) remains valid also in higher order, whereas (13) is modified and usually written as

$$M_W^2 \sin^2\theta_W = M_Z^2 \cos^2\theta_W \sin^2\theta_W = \frac{A}{1-\Delta r}\,. \tag{18}$$

The radiative correction Δr contains the photon vacuum polarization and the genuine weak corrections which depend on all parameters of the model, in particular also on the mass of the Higgs boson M_H and the top quark m_t which do not enter the tree level result (13). (For more details see section 5 and contribution on "Δr"). It should be noted, however, that $\sin^2\theta_W$ as derived from (18) for a given Z mass is not the effective mixing angle in the neutral current vector couplings at the Z peak. The coupling constants get additional contributions by $\gamma - Z$ mixing and vertex corrections (see sections 4.2 and 4.3).

[1] the parameters and their errors for the determination of G_μ from (12) are taken from Particle Data 1988 [18]

2.3 Cross section for $e^+e^- \to f\bar{f}$

Without neclecting terms from the final fermion mass m_f the differential cross section can be written in the following way, where the color factor $N_C^f = 1$ (leptons), $N_C^f = 3$ (quarks) distinguishes between the final state fermions:
($\theta = \angle(e^-, f)$, $\mu_f = m_f^2/s$), $s = (p_- + p_+)^2$)

$$\begin{aligned}\frac{d\sigma}{d\Omega} &= \frac{\alpha^2}{4s} N_C^f \sqrt{1-4\mu_f}\cdot \\ &\cdot\left\{G_1(s)(1+\cos^2\theta) + 4\mu_f G_2(s)\sin^2\theta + \sqrt{1-4\mu_f}\,G_3(s)\cdot 2\cos\theta\right\}\end{aligned} \tag{19}$$

The vector and axial vector coupling constants (9) and the propagator in the lowest order Breit-Wigner approximation

$$\chi_0(s) = \frac{s}{s - M_Z^2 + iM_Z\Gamma_Z^0} \tag{20}$$

with

$$\Gamma_Z^0 = \sum_f N_C^f \frac{\alpha}{3} M_Z \sqrt{1-4\mu_f}\,\left(v_f^2(1+2\mu_f) + a_f^2(1-4\mu_f)\right) \tag{21}$$

determine the functions in the expression (19) as follows:

$$\begin{aligned}G_1(s) &= Q_f^2 - 2v_e v_f Q_f \,\mathrm{Re}\,\chi_0(s) + (v_e^2+a_e^2)(v_f^2+a_f^2-4\mu_f a_f^2)\mid\chi_0(s)\mid^2 \\ G_2(s) &= Q_f^2 - 2v_e v_f Q_f \,\mathrm{Re}\,\chi_0(s) + (v_e^2+a_e^2)v_f^2 \mid\chi_0(s)\mid^2 \\ G_3(s) &= -2a_e a_f Q_f \,\mathrm{Re}\,\chi_0(s) + 4v_e a_e v_f a_f \mid\chi_0(s)\mid^2\,.\end{aligned} \tag{22}$$

These expressions correspond to the Z and photon exchange diagrams. Higgs exchange can be neglected because of the small Yukawa coupling to the electron.

The finite mass terms are only of marginal importance for the known fermions. The tree level formulae given above, however, are also valid for heavy fermion production such as $e^+e^- \to t\bar{t}$.

3 Renormalization

3.1 General remarks

The tree level Lagrangian of the minimal SU(2)×U(1) model involves a certain number of free parameters which are not fixed by the theory. The parameters (or appropriate combinations) can be determined from specific experiments with help of the theoretical results for cross sections and lifetimes. After this procedure of defining the physical input other observables can be calculated allowing verification or falsification of the theory by comparison with the corresponding experimental results.

In higher order perturbation theory not only the predictions for all observables are modified but also the relations between the formal input parameters and their defining experiment are different from the tree level relations in general. Moreover, the procedure is obscured by the appearence of divergences in the higher order contributions

which have to be subtracted in a way consistent with the physical interpretation of the parameters. This operation leads to a redefinition of the parameters in the Lagrangian by an infinite amount. Therefore we abandon the use of the parameters in the original "bare" Lagrangian, the "bare" parameters, and express everything in terms of finite "renormalized" parameters (which can be measured) and counter terms which absorb the divergent parts of the loop contributions. Although this would be sufficient to obtain finite S-matrix elements the off-shell Green functions are not finite by themselves even after this renormalization. This reflects the feature that amplitudes of "bare" fields between the vacuum and one-particle states are not the wave functions normalized to unity, due to the presence of self interactions. In order to obtain finite propagators and vertices also the bare fields in $\mathcal{L}$ have to be redefined in terms of renormalized fields. In this way the "bare" Lagrangian is split into a "renormalized" Lagrangian and a counter term Lagrangian which renders the results for all Green functions in a given order finite. Formally this is done by multiplicative renormalization for each field

$$\phi \rightarrow \sqrt{Z_2}\,\phi$$

and for each parameter in $\mathcal{L}$

$$g \rightarrow Z_1\, g$$

with renormalization constants

$$Z_i = 1 + \delta Z_i.$$

The simplest way to obtain a set of finite Green functions consists in the "minimal subtraction scheme" where (in dimensional regularization) the singular part of each divergent diagram is subtracted and the parameters are defined at a certain renormalization mass scale μ. This scheme has become popular in QCD where due to the absence of free fundamental particle states there is no preference for a specific mass scale in the renormalization procedure.

This situation is different in QED and in the electroweak theory. There the classical Thomson scattering and the particle masses set natural scales where the parameters can be defined. In QED the favoured renormalization scheme is the on-shell scheme where $e = \sqrt{4\pi\alpha}$ and the electron, muon, ... masses are used as input parameters. The finite parts of the counter terms are fixed by the renormalization conditions that the fermion propagators have poles at their physical masses, and e becomes the $ee\gamma$ coupling constant in the Thomson limit of Compton scattering. The extraordinary meaning of the Thomson limit for the definition of the renormalized coupling constant is elucidated by the theorem that the exact Compton cross section at low energies becomes equal to the classical Thomson cross section. In particular this means that e resp. α is free of infrared corrections, and that its numerical value is independent of the order of perturbation theory, only determined by the accuracy of the experiment.

The direct and most natural extension of this QED on-shell scheme leads to the on-shell scheme of the electroweak SU(2)×U(1) theory which was proposed first by Ross and Taylor [19]. Since e and the particle masses are singularly distinguished parameters the physical content becomes best transparent in terms of the set

$$e,\ M_W,\ M_Z,\ M_H,\ m_f \tag{23}$$

as input parameters, together with the physical fields

$$W^{\pm}_{\mu},\ Z_{\mu},\ A_{\mu}$$

from (2) and (3).

Since, for doublet Higgses, there is no room for the mixing angle θ_W as an independent quantity one can use the simplest definition in terms of the physical W and Z masses

$$\sin^2\theta_W = 1 - \frac{M_W^2}{M_Z^2} \equiv s_W^2 \tag{24}$$

as has been proposed by Sirlin [20]. This definition is independent of a specific process and is valid to all orders of perturbation theory.

The advantages of the on-shell renormalization scheme are obvious:

- The parameters have a clear physical meaning and can be measured directly in suitable experiments.
- The parameters (except M_H and m_t) are experimentally known.
- The Thomson cross section from which α is obtained is exact to all orders of perturbation theory.
- The one-loop corrections to $e^+e^- \rightarrow f\bar{f}$ can be naturally separated into "QED corrections" (which means bremsstrahlung type corrections) and "non-QED" or "weak corrections". This feature is of importance for the implementation of higher order contributions into Monte Carlo programs. Moreover, the bulk of QED corrections comes from the infrared soft photons which couple with the Thomson α to the charged fermion currents.

A conceptual problem seems to arise with the light quark mass parameters as input since neither their precise values nor their physical meaning are unambigously known. Fortunately, in our weak radiative corrections they appear only in the vector boson self energies where their contribution can be replaced by the experimentally known cross section for $e^+e^- \rightarrow hadrons$ via a dispersion relation. All other finite mass terms are of order m_f^2/M_Z^2 and vanish in the light quark limit.

Up to now we have not utilized the precisely known G_μ. It is, however, straightforward to calculate G_μ in terms of the on-shell parameters; effectively, this replaces M_W in favor of G_μ, as indicated in section 2.2, by means of eqs. (14) and (18).

Papers concerning e^+e^- processes in the on-shell scheme are: the calculation of the radiative corrections to $e^+e^- \rightarrow \mu^+\mu^-$, first performed by Passarino and Veltman [21] for the range outside the Z resonance; with restriction to the electromagnetic subclass by Greco, Pancheri, Srivastava [22], Berends, Kleiss, Jadach [23], and Böhm, Hollik [24]; the complete one-loop calculation for the PETRA/PEP energy range by Böhm, Hollik [25] and the corresponding calculation of the weak subclass by Brown, Decker, Paschos [26]; the inclusion of the resonance range by Wetzel [27], Lynn, Stuart [28], Hollik [29], Lynn, Peskin, Stuart [30], Consoli, Sirlin [31], Kennedy and Lynn [32], and Bardin et al. [33]. An analytic calculation of the QED corrections in $O(\alpha)$ has been performed by Bardin et al. in [34].

3.2 Renormalization conditions

The importance of the counter terms is twofold:
(i) to absorb the singular parts resulting from the loop integrals and hence to make the expressions finite;
(ii) to define the physical meaning of the involved parameters and hence to complete the definition of the theory.

The renormalization conditions are those conditions which ensure that the input parameters have the values known from the corresponding experiments. In the on-shell scheme they can be separated into two classes: the on-shell subtraction of the self energies making the particle content of the model evident, and the generalization of the electromagnetic charge renormalization.

3.2.1 On-shell subtractions

Since the particle masses are defined as the pole positions of the corresponding propagators (real parts) we are primarily concerned with the system of the gauge boson propagators. In lowest order the neutral boson propagator matrix is diagonal after diagonalizing the mass matrix by the transformation (3). But mixing at the quantum level prohibits the γ and Z from propagating independently of each other. Consequently, the propagator of the neutral boson system has to be considered as a 2×2 matrix. The one-loop corrections can be collected by the self energy functions Σ_{ij} (defined as the amputated one-particle irreducible 2-point functions) yielding the inverse propagator matrix (for light external fermions we need only the transverse part $\sim g_{\mu\nu}$)

$$\begin{pmatrix} s+\Sigma_{\gamma\gamma}(s) & \Sigma_{\gamma Z}(s) \\ \Sigma_{\gamma Z}(s) & s-M_{Z0}^2+\Sigma_{ZZ}(s) \end{pmatrix} \tag{25}$$

Inverting this matrix yields the following structure of the neutral boson propagators:

$$D_\gamma(s) = \frac{1}{s+\Sigma_{\gamma\gamma}(s)-(\Sigma_{\gamma Z}(s))^2/[s-M_{Z0}^2+\Sigma_{ZZ}(s)]} \tag{26}$$

$$D_{\gamma Z}(s) = -\frac{\Sigma_{\gamma Z}(s)}{[s+\Sigma_{\gamma\gamma}(s)][s-M_{Z0}^2+\Sigma_{ZZ}(s)]-(\Sigma_{\gamma Z}(s))^2} \tag{27}$$

$$D_Z(s) = \frac{1}{s-M_{Z0}^2+\Sigma_{ZZ}(s)-(\Sigma_{\gamma Z}(s))^2/[s+\Sigma_{\gamma\gamma}(s)]} \tag{28}$$

Moreover, we have the W propagator

$$D_W(s) = \frac{1}{s-M_{W0}^2+\Sigma_{WW}(s)}. \tag{29}$$

This form of the propagators corresponds to the geometrical summation of the iterated 1PI insertions. At the one-loop level the products of higher orders in the propagators do not contribute.

The mass parameters in D_W and D_Z are the "bare" masses of the unrenormalized Lagrangian. They are different from the physical masses M_W, M_Z because the corresponding denominators do not vanish at $s=M_{W0}^2$ resp. $s=M_{Z0}^2$. The physical masses

can be introduced together with the mass counter terms $\delta M_{W,Z}^2$ as follows:

$$\begin{aligned} M_{W0}^2 &= M_W^2+\delta M_W^2 \\ M_{Z0}^2 &= M_Z^2+\delta M_Z^2 . \end{aligned} \tag{30}$$

The counter terms are fixed by the renormalization conditions that the real parts of the denominators in (28) and (29) have zeros at $s=M_{W,Z}^2$.

In this way two of our input parameters and their counter terms have been defined.

3.2.2 Charge renormalization

Our third physical input parameter is the electromagnetic charge $e=\sqrt{4\pi\alpha}$. The defining condition is

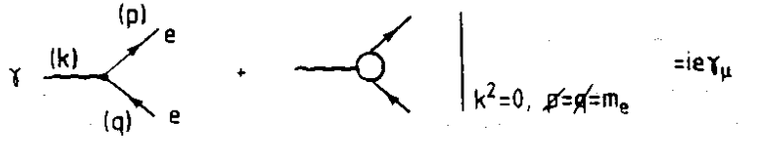

where the bubble denotes all one-loop contributions to the electromagnetic vertex of the electron

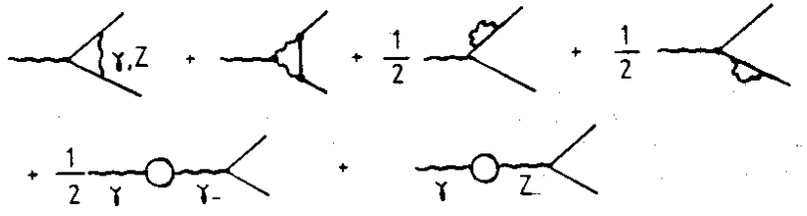

and the "bare" vertex is evaluated with the "bare" charge

$$e_0 = e+\delta e$$

The charge counter term δe is then fixed by the condition above, and e_0 can be replaced by the physical quantity e.

3.3 Field renormalization

Although the method outlined above would be sufficient to obtain finite S -matrix elements the propagators and vertices themselves are not yet finite. For this aim we have also to perform field renormalization as indicated in 3.1. Leading to the same **physical** results in a given order, various book-keeping strategies have been applied in the literature where the corresponding propagators and vertex form factors are quite different. According to similar treatments the following classification can be made:

Lynn, Stuart [28] and Böhm, Hollik, Spiesberger [35]:
A single field renormalization constant is introduced for each symmetry multiplet of vector fields:

$$\vec{W}_\mu \to \sqrt{Z_W}\,\vec{W}_\mu, \quad B_\mu \to \sqrt{Z_B}\,B_\mu .$$

The introduction of field renormalization in the Lagrangian corresponds to a second subtraction in the self energies (after the on-shell subtraction). The two constants Z_W and Z_B are sufficient to make the self energies (resp. the propagators) and the vertex corrections finite. These additional two field renormalization constants allow to fulfil the further two renormalization conditions:
vanishing of the γZ mixing propagator for real photons ($s = 0$); residue = 1 for the photon propagator (in analogy to pure QED). The residues of the W and Z propagators, however, are different from unity.

Aoki et al. [36], Fleischer and Jegerlehner [37], and Bardin et al. [38]:
An individual field renormalization constant is introduced for the the photon, Z, W fields as well as for the photon-Z mixing. This method allows in addition to require residue = 1 for the W and Z propagators as well.

Kennedy and Lynn [32] do not make use of field renormalization but combine the propagators (which are not finite by themselves) with the coupling constants attached to their end points in physical matrix elements. In this way running parameters are introduced which absorb the infinities in the 2-point functions. After introducing the physical input at a given q^2 scale (in practice at $M_{W,Z}$ and the Thomson scale) also the finite parts are fixed.

The calculation of Bardin et al. [34,38] has been performed in the unitary gauge. This is the reason why, although applying field renormalization, their individual propagators and vertices are not finite. Those specific combinations, however, which enter the one-loop matrix elements for physical processes are again finite.

In the following we refer mainly to the results obtained by the scheme applied in [35], see also [39,40]. A discussion of the relation to the scheme of [32] is given below in section 4.5.

For the details in performing the renormalization we refer to the literature [35,40]. The results can be summarized in terms of dressed renormalized gauge boson propagators and gauge boson - fermion vertices where the photonic part which is IR divergent can be split off and has the same analytic form as in QED. This part will be combined with real bremsstrahlung in order to obtain a result which is also IR finite (this defines the "QED corrections"). The rest, the "weak corrections", are all finite by themselves, expressed in terms of our physical input parameters, and can be used as the building blocks for calculating all the 4-fermion processes of interest. Here we want to concentrate primarily on e^+e^- annihilation.

4 Results for e^+e^- processes

4.1 General structure of radiative corrections in $e^+e^- \to f\bar{f}$

As indicated in the description of the on-shell renormalization scheme in section 3.2 the one-loop corrections to the process $e^+e^- \to f\bar{f}$ can be subdivided quite naturally into the following subclasses:

- "QED corrections", which consist of those diagrams with an extra photon added to the Born diagrams either as a real bremsstrahlung photon or a virtual photon loop. They are depicted in Figure 1. Although considered not very interesting with respect to the underlying theory they are in general large at LEP energies and hence need a lot of attention for practical purposes.

- "Weak corrections", which collect all other one-loop diagrams: The subset of diagrams which involve corrections to the vector boson propagators γ, Z (Figure 2), the set of vertex corrections (where the virtual photon contributions have been removed) and box diagrams with two massive boson exchange (Figure 3).

The separation of the QED corrections is sensible since they form a gauge invariant subset and depend on the details of the experiments via the cuts applied to the final state photon. Their proper treatment constitutes the link between data taking and physics analysis. The infrared finite weak corrections are independent of experimental cuts; they include the more subtle part of the electroweak theory beyond the tree level and are also sensitive to "new physics" objects.

Due to the smallness of the electron mass the lowest order Higgs exchange diagram can be neglected. For the same reason also diagrams with Higgs - gauge boson mixing and box diagrams where one or both of the internal vector bosons of Figure 3 are replaced by Higgs scalars are negligible; they are suppressed by at least a factor $\frac{\alpha}{\pi}\frac{m_e}{M_W}$. The propagator corrections, however, involve all particles of the model, in particular the as yet unknown Higgs boson and the top quark, and thus depend on M_H and m_t. For light final fermions ($f \neq b,t$) the vertex corrections of Figure 3 contain only W and Z in virtual states. Vertex corrections to heavy fermions depend also on the Higgs-fermion Yukawa couplings.

The tree level formulae of 2.3 are valid also for a $t\bar{t}$ final state. In the present context we want to restrict ourselves to the situation where only the known fermions appear as external particles for which the one-loop corrections can be cast into a compact and transparent form. Since the m_f terms give only a very small contribution already at the tree level we can neglect all fermion mass effects in the next order vertex and box diagrams with two exceptions: (i) mass terms from a virtual top quark are always treated without approximation; (ii) in the QED corrections all mass terms (also from light fermions) are kept which would lead to mass singularities for $m_f \to 0$.

In this approximation the vertex corrections can be represented in terms of form factors $F_{V,A}^{Z(\gamma)f}(k^2)$ for the vector and axial vector currents only. Also the box diagrams can be written as a sum over terms like

(initial current) · (final current) · (formfactor).

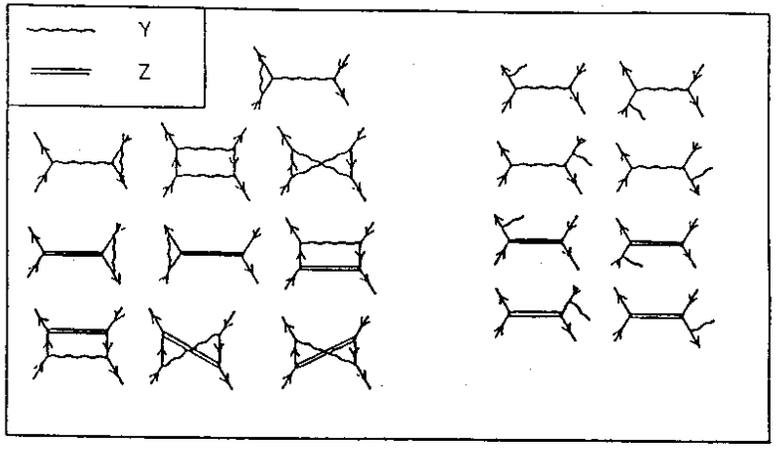

Figure 1: QED corrections to $e^+e^- \to \mu^+\mu^-$

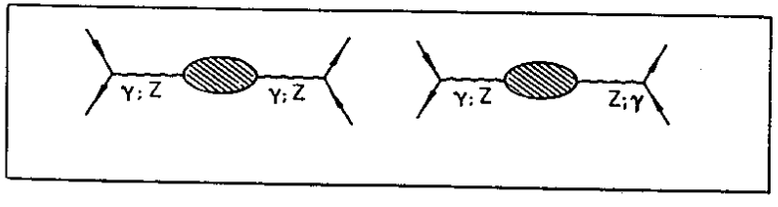

Figure 2: Propagator corrections to $e^+e^- \to \mu^+\mu^-$

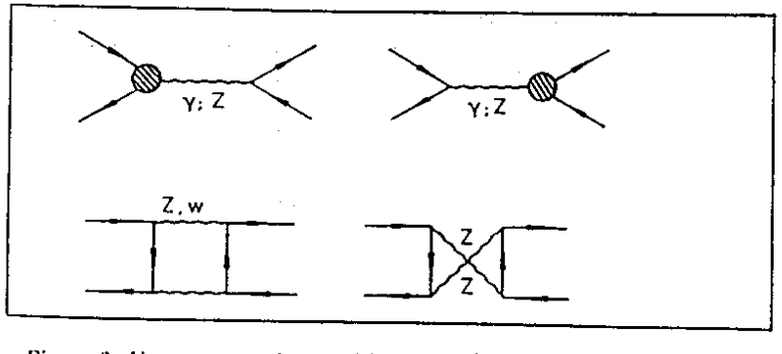

Figure 3: Vertex corrections and box contributions to $e^+e^- \to \mu^+\mu^-$

where the currents have only vector and axial vector contributions. This simple structure arises from helicity conservation at the vector boson - fermion vertices in the small mass limit. It allows to express the corrected cross section in the same way as given in (19); only the invariant functions in (22) which are not already suppressed in (19) by an overall factor of m_f^2/s have to be substituted by the versions with corrected propagators and coupling constants.

After this general discussion we give concrete specifications of the various ingredients in the one-loop cross section.

4.2 The propagator corrections

The self energy insertions in the 2-point functions yield the dressed renormalized propagators. The propagator corrections are frequently also called "oblique" corrections [30]. The dressed W, Z, γ propagators contain the renormalized 1-particle irreducible (1PI) one-loop self energies, denoted by a $\hat{}$, in the following way:

$$\hat{D}_W(s) = \frac{1}{s - M_W^2 + \hat{\Sigma}_{WW}(s)} \tag{31}$$

$$\hat{D}_Z(s) = \frac{1}{s - M_Z^2 + \hat{\Sigma}_{ZZ}(s) - \frac{\hat{\Sigma}_{\gamma Z}(s)^2}{s + \hat{\Sigma}_{\gamma\gamma}(s)}} \tag{32}$$

$$\hat{D}_\gamma(s) = \frac{1}{s + \hat{\Sigma}_{\gamma\gamma}(s) - \frac{\hat{\Sigma}_{\gamma Z}(s)^2}{s - M_Z^2 + \hat{\Sigma}_{ZZ}(s)}} \tag{33}$$

We also have the non-diagonal γZ mixing propagator

$$\hat{D}_{\gamma Z}(s) = -\frac{\hat{\Sigma}_{\gamma Z}(s)}{[s + \hat{\Sigma}_{\gamma\gamma}(s)][s - M_Z^2 + \hat{\Sigma}_{ZZ}(s)] - \hat{\Sigma}_{\gamma Z}(s)^2} \tag{34}$$

This form is quite similar to (26) - (29), but now due to field renormalization ($\equiv$ double-subtraction) the self energies are finite. The renormalized self energies can be expressed in terms of the non-renormalized ones as follows [40]:

$$\begin{aligned}
\hat{\Sigma}_{\gamma\gamma}(s) &= \Sigma_{\gamma\gamma}(s) - s\,\Sigma'_{\gamma\gamma}(0) \\
\hat{\Sigma}_{\gamma Z}(s) &= \Sigma_{\gamma Z}(s) - \Sigma_{\gamma Z}(0) + s\left\{\frac{2\Sigma_{\gamma Z}(0)}{M_Z^2} - \frac{c_W}{s_W}\left(\frac{\delta M_Z^2}{M_Z^2} - \frac{\delta M_W^2}{M_W^2}\right)\right\} \\
\hat{\Sigma}_{ZZ}(s) &= \Sigma_{ZZ}(s) - \delta M_Z^2 + \delta Z_1^Z\,(s - M_Z^2) \\
\hat{\Sigma}_{WW}(s) &= \Sigma_{WW}(s) - \delta M_W^2 + \delta Z_1^W\,(s - M_W^2)
\end{aligned} \tag{35}$$

with

$$\begin{aligned}
\delta Z_1^Z &= -\Sigma'_{\gamma\gamma}(0) - 2\,\frac{c_W^2 - s_W^2}{s_W c_W}\,\frac{\Sigma_{\gamma Z}(0)}{M_Z^2} + \frac{c_W^2 - s_W^2}{s_W^2}\left(\frac{\delta M_Z^2}{M_Z^2} - \frac{\delta M_W^2}{M_W^2}\right) \\
\delta Z_W^2 &= -\Sigma'_{\gamma\gamma}(0) - 2\,\frac{c_W}{s_W}\,\frac{\Sigma_{\gamma Z}(0)}{M_Z^2} + \frac{c_W^2}{s_W^2}\left(\frac{\delta M_Z^2}{M_Z^2} - \frac{\delta M_W^2}{M_W^2}\right)
\end{aligned}$$

$$\delta M_W^2 = \mathrm{Re}\,\Sigma_{WW}(M_W^2)$$
$$\delta M_Z^2 = \mathrm{Re}\left(\Sigma_{ZZ}(M_Z^2) - \frac{\hat{\Sigma}^2_{\gamma Z}(M_Z^2)}{M_Z^2 + \hat{\Sigma}_{\gamma\gamma}(M_Z^2)}\right).$$

In the following we also make use of the dimensionless quantities

$$\Pi_{\gamma\gamma}(s) = \frac{\hat{\Sigma}_{\gamma\gamma}(s)}{s} \qquad (36)$$
$$\Pi_{\gamma Z}(s) = \frac{\hat{\Sigma}_{\gamma Z}(s)}{s}.$$

The unrenormalized self energies are listed in the Appendix. They contain the contributions from the presently experimentally unknown particles Higgs and top. But also all kind of "new physics" objects with couplings exclusively to the gauge bosons can easily be incorporated in the propagators (31) - (34) just by augmenting the unrenormalized self energies by the addditional diagrams and applying (35) (as far as the new objects preserve the SU(2)×U(1) tree level structure).

Dressing the propagators by means of (32) - (34) leads to the following structure of the e^+e^- amplitude, depicted graphically with the following signature:
- double shaded blob: full propagators,
- single shaded blobs: 1PI self energies,
- photon line with a dot: photon propagator dressed by vacuum polarization.

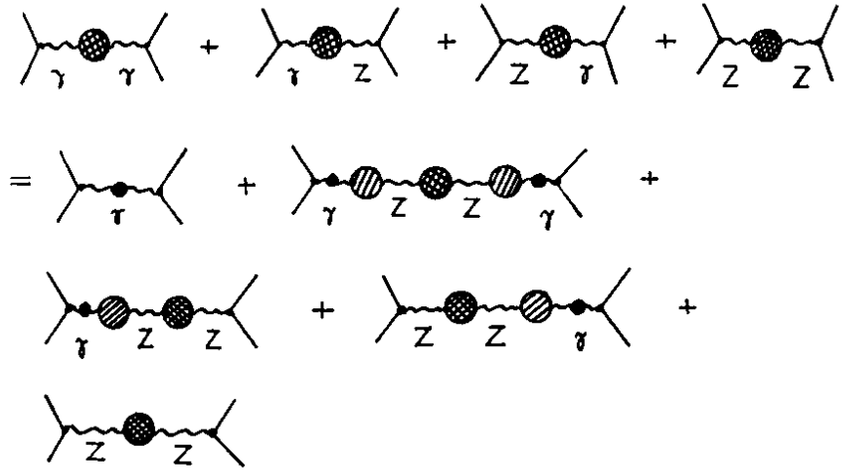

The corresponding analytical expressions allow the following simple interpretation:

4.2.1 photon exchange:

$$= Q_e Q_f \frac{e^2}{1 - \Pi_{\gamma\gamma}(s)} \cdot \frac{1}{s} \qquad (37)$$
$$\approx Q_e Q_f \frac{e^2(s)}{s}.$$

Thereby the real part $\mathrm{Re}\Pi_{\gamma\gamma}$, which is 0.06 for $s \approx M_Z^2$, has been absorbed by defining a running electric charge

$$e^2(s) = \frac{e^2}{1 + \mathrm{Re}\,\Pi_{\gamma\gamma}(s)}. \qquad (38)$$

Dealing with the running charge is equivalent to the γ self energy insertion in the photon propagator where the imaginary part $\mathrm{Im}\Pi_{\gamma\gamma}(s) \approx -0.02$ around the Z mass has been neglected.

4.2.2 Z boson exchange:

With the abbreviation

$$\Sigma_Z(s) = \hat{\Sigma}_{ZZ}(s) - \frac{\hat{\Sigma}_{\gamma Z}(s)^2}{s + \hat{\Sigma}_{\gamma\gamma}(s)} \qquad (39)$$

and the initial (e) and final (f) current matrix elements (u and v denote the external spinors)

$$J^{(e)} = \bar{v}_e \left[\gamma_\mu (I_3^e - 2s_W^2 Q_e) - \gamma_\mu\gamma_5 I_3^e\right] u_e \qquad (40)$$
$$J^{(f)} = \bar{u}_f \left[\gamma_\mu (I_3^f - 2s_W^2 Q_f) - \gamma_\mu\gamma_5 I_3^f\right] v_f$$

the diagonal Z propagator diagram has the following form:

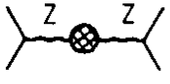

$$= \frac{e^2}{4s_W^2 c_W^2} \cdot \frac{J^{(e)} \cdot J^{(f)}}{s - M_Z^2 + \Sigma_Z(s)} \qquad (41)$$
$$= \frac{e^2}{4s_W^2 c_W^2} \cdot \frac{J^{(e)} \cdot J^{(f)}}{(s - M_Z^2)[1 + \Pi_Z(s)] + i\,\mathrm{Im}\,\Sigma_Z(s)}$$
$$= \frac{e^2}{4s_W^2 c_W^2} \cdot \frac{1}{1 + \Pi_Z(s)} \cdot \frac{J^{(e)} \cdot J^{(f)}}{s - M_Z^2 + i\,\mathrm{Im}\Sigma_Z(s)/[1 + \Pi_Z(s)]}$$

where

$$\mathrm{Re}\,\Sigma_Z(s) = (s - M_Z^2)\,\Pi_Z(s). \qquad (42)$$

(Note that $\mathrm{Re}\Sigma_Z(M_Z^2) = 0$ due to the on-shell subtraction).

Over the energy range of the Z peak the s dependence can, to a sufficiently good approximation, be simplified in the following way:

$$\frac{e^2}{4s_W^2 c_W^2} \cdot \frac{1}{1 + \Pi_Z(M_Z^2)} \cdot \frac{J^{(e)} \cdot J^{(f)}}{s - M_Z^2 + i\,\frac{s}{M_Z^2} \cdot \frac{\mathrm{Im}\,\Sigma_Z(M_Z^2)}{1 + \Pi_Z(M_Z^2)}}. \qquad (43)$$

Let us now interpret the various terms in (43):

The **imaginary part** of the denominator is related to the physical Z width Γ_Z determined in $O(\alpha^2)$ as follows:

$$M_Z \Gamma_Z = \frac{\mathrm{Im}\Sigma_Z(M_Z^2) + M_Z \Delta\Gamma_Z}{1 + \Pi_Z(M_Z^2)}. \tag{44}$$

The term $\Delta\Gamma_Z$ summarizes all $O(\alpha^2)$ contributions to the width which are not already contained in the 2-point functions. These are:
- weak corrections to the decays $Z \to f\bar{f}$;
- QED corrections to the decays $Z \to f\bar{f}$, $f \neq \nu$;
- QCD corrections to the decays $Z \to q\bar{q}$;
- other decay channels of higher order in the coupling constants. In practice only the decay $Z \to \sum_f Hf\bar{f}$ is of some importance for a light Higgs (≈ 5 MeV for $M_H = 10$ GeV); other decay channels can be neglected (see the contribution to this report by van der Bij, Glover et al.).

With the weak form factors $F_{V,A}^{Zf}$ of section 4.3 we can write for $\Delta\Gamma_Z$ [2]

$$\begin{aligned}\Delta\Gamma_Z &= \sum_f N_C^f \frac{2}{3}\alpha M_Z \left[v_f \,\mathrm{Re}F_V^{Zf}(M_Z^2) + a_f \,\mathrm{Re}F_A^{Zf}(M_Z^2)\right] \\ &+ \sum_f N_C^f \frac{\alpha}{3} M_Z (v_f^2 + a_f^2)\cdot\delta_{QED} \\ &+ \sum_{f=q} N_C^f \frac{\alpha}{3} M_Z (v_f^2 + a_f^2)\cdot\delta_{QCD} \\ &+ \sum_f \Gamma(Z \to Hf\bar{f}),\end{aligned} \tag{45}$$

together with (massless fermion limit)

$$\delta_{QED} = \frac{3\alpha}{4\pi} Q_f^2 \tag{46}$$

$$\delta_{QCD} = \frac{\alpha_s(M_Z^2)}{\pi} + 1.405\left(\frac{\alpha_s(M_Z^2)}{\pi}\right)^2 \tag{47}$$

and $\Gamma(Z \to Hf\bar{f})$ taken from [41]. Taking into account the mass dependence of the QCD corrections in the partial width for $Z \to b\bar{b}$ increases Γ_Z by 2 MeV if $\alpha_s(M_Z^2) = 0.11 \pm 0.01$ [42] is used. The uncertainty from α_s induces an uncertainty in the total width of about ± 6 MeV.

The **real part** in the denominator of (43), which is associated with Π_Z, can be interpreted as a modification of the effective NC coupling constant. For general s the quantity

$$\frac{e^2}{4 s_W^2 c_W^2}\cdot\frac{1}{1 + \Pi_Z(s)} \tag{48}$$

acts as an effective running NC coupling strength, in analogy to $e^2(s)$ in the QED part of the amplitude.

[2] we have assumed that $2m_t > M_Z$

For the physical understanding it is helpful to present explicitly the leading terms of the quantity $\Pi_Z(s)$ which are due to the light fermions appearing in terms of the γ vacuum polarization, and to a possibly heavy top quark:

$$\Pi_Z(s) = -\Delta\alpha + \frac{c_W^2 - s_W^2}{s_W^2}\Delta\bar{\rho} + \cdots \tag{49}$$

where

$$\Delta\alpha = -\,\mathrm{Re}\,\Pi_{\gamma\gamma}(M_Z^2), \tag{50}$$

$$\Delta\bar{\rho} = \frac{\alpha}{4\pi}\cdot\frac{3}{4 s_W^2 c_W^2}\left(\frac{m_t}{M_Z}\right)^2. \tag{51}$$

$\Delta\bar{\rho}$ is also the leading term coming from a heavy top in the quantity [43]

$$1 + \frac{\Sigma_{ZZ}(0)}{M_Z^2} - \frac{\Sigma_{WW}(0)}{M_W^2} \tag{52}$$

which enters the NC/CC ratio in neutrino scattering, commonly known as the "ρ parameter". Since this leading term is independent of s it enters both $\Pi_Z(s)$ and the ρ parameter as a constant, but with different coefficients.

The appearance of the photon vacuum polarization in (43) rescales $e^2(0)$ to $e^2(M_Z^2)$ around the Z peak. But in contrast to the effective coupling in the γ exchange amplitude, where a heavy top decouples, we have an increasing contribution in the Z exchange diagram for large m_t. For sufficiently small m_t, however, the main effect is obtained by $e^2 \to e^2(M_Z^2)$.

For the correct top mass dependence we have to take care also of the variation of s_W^2 with m_t when it is calculated from the G_μ constraint (18) with help of Δr. Utilizing (18) in order to eliminate the combination $e^2/s_W^2 c_W^2$ in (43), together with the leading behaviour of Δr (see section 5)

$$\Delta r = \Delta\alpha - \frac{c_W^2}{s_W^2}\Delta\bar{\rho} + \ldots \tag{53}$$

and Π_Z from (49) yields:

$$\begin{aligned}\frac{e^2}{4 s_W^2 c_W^2}\cdot\frac{1}{1 + \Pi_Z(s)} &= \sqrt{2} G_\mu M_Z^2 \frac{1 - \Delta r}{1 + \Pi_Z(s)} \\ &= \sqrt{2} G_\mu M_Z^2 [1 + \Delta\bar{\rho} + \cdots].\end{aligned} \tag{54}$$

The appearance of the ρ parameter in (54) can physically be understood by the introduction of the CC coupling strength (the G_μ) in our NC amplitude (41). The complete correction factor, together with the approximate leading form given in (54), is displayed in Figure 4. As one can see, the difference is smaller than 0.005.

A last remark concerns the effect of the $(\Pi_{\gamma Z})^2$ term in (32): it contributes a next order term to Π_Z of the form [3]

$$-\frac{c_W^4}{s_W^4}(\Delta\bar{\rho})^2 \tag{55}$$

which is, however, cancelled in (54), since the same additional term appears in Δr as well (with the opposite sign).

[3] this is due to the counter term in the renormalised mixing (35)

4.2.3 γZ mixing

The appearance of γZ mixing beyond the tree level may either be viewed as an additional non-diagonal propagator or as a redefinition of the NC vector coupling constants v_f, a_f from eq. (9). According to the latter point of view, we can write

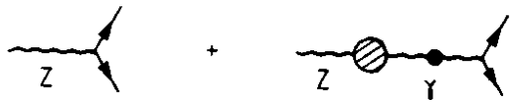

$$= \gamma_\mu (v_f - a_f\gamma_5) + \gamma_\mu Q_f \frac{\Pi_{\gamma Z}(s)}{1+\Pi_{\gamma\gamma}(s)} \tag{56}$$

$$= \gamma_\mu \left[\frac{I_3^f - 2s_W^2 Q_f}{2s_W c_W} + Q_f \frac{\Pi_{\gamma Z}(s)}{1+\Pi_{\gamma\gamma}(s)} \right] - \frac{I_3^f}{2s_W c_W}\gamma_\mu\gamma_5$$

$$= \frac{1}{2s_W c_W}\left\{ \gamma_\mu \left[I_3^f - 2Q_f \left(s_W^2 - s_W c_W \frac{\Pi_{\gamma Z}(s)}{1+\Pi_{\gamma\gamma}(s)} \right) \right] - I_3^f \gamma_\mu\gamma_5 \right\}. \tag{57}$$

The structure of this term allows an absorption in an effective mixing angle $\bar{s}_W^2$ which is a universal quantity, i.e. it is independent of the external fermions:

$$\bar{s}_W^2 = s_W^2 - c_W s_W \,\mathrm{Re}\, \frac{\Pi_{\gamma Z}(s)}{1+\Pi_{\gamma\gamma}(s)}. \tag{58}$$

In order to obtain a real mixing angle we had to omit the imaginary part (which is ≈ -0.01 for $s = M_Z^2$, independent of M_H and practically also of m_t). With (58), evaluated at $s = M_Z^2$, the effective Z exchange amplitude near the peak can be written as

$$\frac{e^2}{4s_W^2 c_W^2} \cdot \frac{1}{1+\Pi_Z(M_Z^2)} \cdot \frac{\bar{J}^{(e)} \cdot \bar{J}^{(f)}}{s - M_Z^2 + i\frac{s}{M_Z^2} M_Z\Gamma_Z} \tag{59}$$

with Γ_Z from (44)-(45) and with the fermionic currents expressed in terms of $\bar{s}_W^2$, taken between the external spinors in analogy to (40):

$$\bar{J}^{(e,f)} = \gamma_\mu \left(I_3^{e,f} - 2Q_{e,f}\,\bar{s}_W^2 \right) - I_3^{e,f}\,\gamma_\mu\gamma_5. \tag{60}$$

For completeness, the imaginary part has to be added by hand in (59) if one prefers to have the effective currents (60) with a real mixing angle:

$$\bar{s}_W^2 \to \bar{s}_W^2 - i\, s_W c_W \,\mathrm{Im}\, \frac{\Pi_{\gamma Z}(s)}{1+\Pi_{\gamma\gamma}(s)}. \tag{61}$$

It is interesting to study the m_t-dependence of $\bar{s}_W^2$, defined in (58), in the leading term for large m_t. With $\Delta\bar{\rho}$ from (51) we find

$$\bar{s}_W^2 = s_W^2 + c_W^2\,\Delta\bar{\rho} + \cdots \tag{62}$$

Figure 5 shows the quantity $\bar{s}_W^2$ and its approximate form given in (62). Having in mind that s_W^2 decreases sizeably for heavy top masses according to eqs. (18) and (53)

$$s_W^2(\text{heavy}) - s_W^2(\text{light}) \approx -\frac{c_W^4}{c_W^2 - s_W^2}\Delta\bar{\rho} \tag{63}$$

the combined net effect in $\bar{s}_W^2$ is given by

$$\bar{s}_W^2(\text{heavy}) - \bar{s}_W^2(\text{light}) \approx -\frac{c_W^2 s_W^2}{c_W^2 - s_W^2}\Delta\bar{\rho}. \tag{64}$$

As the comparison with (63) shows, the m_t-dependence of $\bar{s}_W^2$ is weaker than that of s_W^2 by a factor $s_W^2/c_W^2 \approx 1/3$.

Let us summarize the propagator corrections as follows:

1. The propagator corrections can be implemented in e^+e^- amplitudes in terms of three 1PI self energy functions

   $$\Pi_{\gamma\gamma}(s),\ \Pi_{\gamma Z}(s),\ \Pi_Z(s),$$

   defined in (36), (42), together with the $O(\alpha^2)$ corrected total Z width Γ_Z given by (44) - (47). These quantities are universal, i.e. they are independent of the species of the external fermions. They can be applied to t-channel exchanges as well. For light external fermions ($f \neq b, t$), where the top quark is not present in the residual vertex and box diagrams and where the Higgs contribution is negligible, these four pieces are the only place where the unknown parameters of the minimal model enter. This applies also to new physics objects within SU(2)×U(1) if they do not couple directly to the external fermions.

2. The amplitude for $e^+e^- \to f\bar{f}$ with dressed propagators is similar to the Born amplitude. It is the sum of the γ exchange diagram, given by (37), and the Z exchange diagram according to the formulae (59) - (61). If the imaginary parts of $\Pi_{\gamma\gamma}$ and $\Pi_{\gamma Z}$ are neglected, the parametrization of the amplitude is equivalent to the use of the "genuine" Born amplitude (which leads us to (22))

   $$Q_e Q_f \frac{e^2}{s} + \frac{e^2}{4s_W^2 c_W^2} \frac{J^{(e)} \cdot J^{(f)}}{s - M_Z^2 + i M_Z \Gamma_Z^0}$$

   with the following replacements:

   $$\begin{aligned}
   \frac{e^2}{s} &\to \frac{e^2(s)}{s} \\
   \frac{e^2}{4s_W^2 c_W^2} &\to \frac{e^2}{4s_W^2 c_W^2} \cdot \frac{1}{1+\Pi_Z(s)} \equiv \sqrt{2} G_\mu M_Z^2 \frac{1-\Delta r}{1+\Pi_Z(s)} \\
   s_W^2 &\to \bar{s}_W^2 \text{ in } J^{(e)} \text{ and } J^{(f)} \\
   M_Z\Gamma_Z^0 &\to \frac{s}{M_Z^2} \cdot M_Z\Gamma_Z
   \end{aligned} \tag{65}$$

For the high accuracy required for LEP experiments the imaginary parts should also be incorporated in the final expresssions. As an example, the imaginary part of $\Pi_{\gamma\gamma}(M_Z^2)$ gives a contribution to the on-resonance forward-backward asymmetry $A_{FB}(M_Z^2)$ in $e^+e^- \to \mu^+\mu^-$ of $\delta A_{FB} = +0.002$. One has to keep in mind, however, that there are also others than propagator corrections, as to be discussed in the following sections 4.3 and 4.4.

We conclude this section with a technical remark. Only the fermion contributions to $\bar{s}_W^2$ defined in (58) (as well as to the normalization of the neutral current strength given in (54)) form a gauge invariant set and as such are physically sensible. Therefore, strictly speaking, one should restrict only to definitions in terms of physical quantities; this means that also others than propagator corrections have to be incorporated which are not of the universal type. However, as explained in section 4.6, all the "physical" definitions of the weak mixing angle (as well as the neutral current strength) from Z processes have the same universal piece which is also the numerically dominant one and contains the unknown physics. For this reason, $\bar{s}_W^2$, defined in (58), and the normalization factor of (54) are useful auxiliary quantities. In this sense, we can also introduce, in analogy to (18), a new quantity $\overline{\Delta r}$ which relates $\bar{s}_W^2$ directly to the Z mass:

$$M_Z^2\, \bar{c}_W^2\, \bar{s}_W^2 = \frac{A}{1-\overline{\Delta r}}. \tag{66}$$

For the leading terms one finds easily with help of (53) and (62):

$$\overline{\Delta r} = \Delta\alpha - \Delta\bar{\rho} + \cdots$$

which in the light fermion part $\Delta\alpha$ is identical to Δr. The top dependence, however, is much weaker due to the missing enhancement factor c_W^2/s_W^2. For a thorough numerical discussion see the "Δr" contribution to this report.

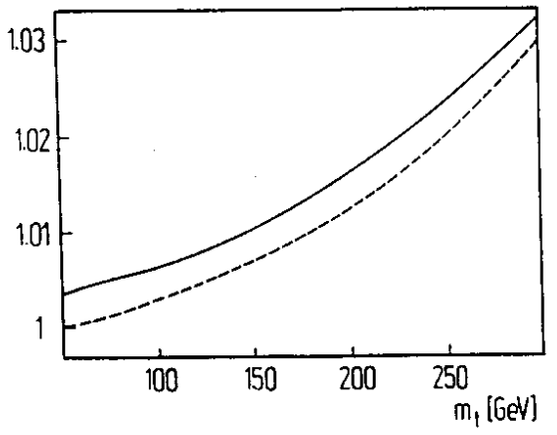

Figure 4:
$(1-\Delta r)/(1+\Pi_Z)$ (solid line) and approximate form (54) (dashed line).
$M_Z = 92$ GeV, $M_H = 100$ GeV.

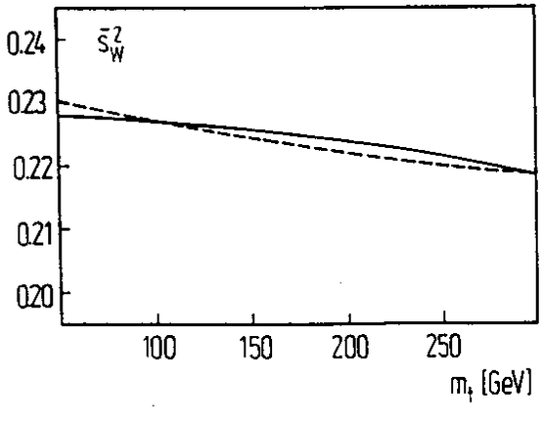

Figure 5:
$\bar{s}_W^2$ from (58) (solid line) and approximate form (62) (dashed line).
$M_Z = 92$ GeV, $M_H = 100$ GeV.

4.3 The vertex corrections

As mentioned in the general classification of section 4.1 the vertex corrections can be summarized in terms of s-dependent vector and axial vector form factors if the masses m_f of the external fermions are small compared to M_W, both for the electromagnetic and the weak NC vertex. In this section we specify more explicitly these form factors and discuss their magnitude and their effects in physical observables of interest in Z physics.

In our terminology, "vertex corrections" denote the $\gamma(Z)ff$ 3-point functions in one-loop order after renormalization, where also the self energy contributions to the external legs have been included. The form factors given here can therefore be used as additive terms to the effective V and A coupling constants in the amplitudes.

In contrast to the propagator corrections the vertex corrections are not universal, depending in general on the fermion species. For this reason we have to list them separately for ν, e, u, d type fermions. In addition, the b quark is exceptional due to the virtual top contributions in the vertex. The vertex correction diagrams are listed in Figure 6. For $f \neq b$ only (a) - (c) have to be taken into account; (d) - (g) are negligible due to small Yukawa couplings (as well as the dropped graphs with internal physical Higgs states).

Our terminology is as follows:

$F_{V,A}^{Zf}$ and $F_{V,A}^{\gamma f}$ denote the IR finite weak (i.e. non-QED resp. non-photonic) form factors for the Zff and γff vertex which, together with the lowest order terms in (18), yield the "dressed" vertices:

$$\begin{aligned}\Gamma_\mu^{Zff} &= ie\gamma_\mu(v_f - a_f\gamma_5)\left[1 + Q_f^2 F_{QED}(s)\right] \\ &\quad + ie\gamma_\mu\left[F_V^{Zf}(s) - F_A^{Zf}(s)\gamma_5\right], \end{aligned} \tag{67}$$

$$\begin{aligned}\Gamma_\mu^{\gamma ff} &= -ieQ_f\gamma_\mu\left[1 + Q_f^2 F_{QED}(s)\right] \\ &\quad - ie\gamma_\mu\left[F_V^{\gamma f}(s) - F_A^{\gamma f}(s)\gamma_5\right]. \end{aligned}$$

The QED contribution from γ exchange is, for $s \gg m_f^2$, contained in the single form factor

$$F_{QED}(s) = \frac{\alpha}{4\pi}\Lambda_1(s, m_f), \tag{68}$$

$$\begin{aligned}\Lambda_1(s, m_f) &= -2\log\frac{s}{\lambda^2}\left(\log\frac{s}{m_f^2} - 1\right) + \log\frac{s}{m_f^2} + \log^2\frac{s}{m_f^2} \\ &\quad + 4\left(\frac{\pi^2}{3} - 1\right) + 2\pi i\left(\log\frac{s}{\lambda^2} - \frac{3}{2}\right).\end{aligned}$$

The IR divergence, regularized by a small photon mass λ, as well as the $\log^2$ -term are cancelled when these virtual QED corrections are combined with the corresponding real photon corrections (after integration over the photon phase space), see Figure 1.

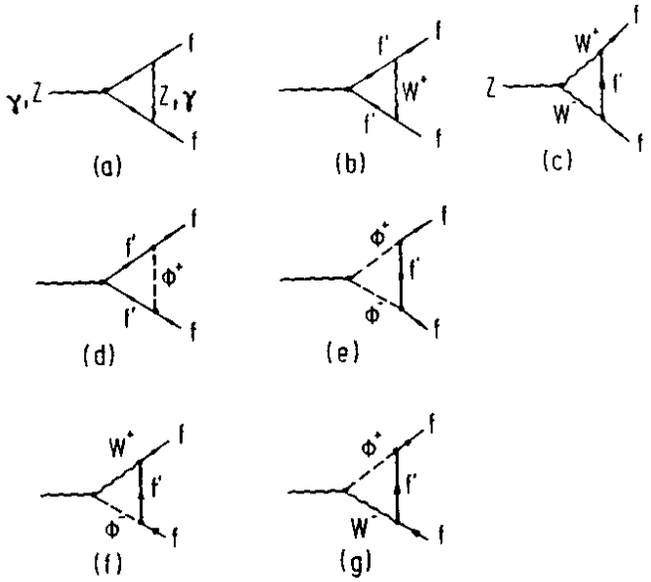

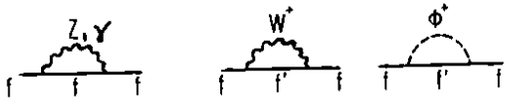

Figure 6:
Vertex corrections and fermion self energy insertions
(neutral Higgs bosons neglected)

Since F_{QED} without real bremsstrahlung is physically meaningless we skip it from our discussion of the pure weak amplitudes. The effects of QED corrections are rather treated in the more specific discussions of the various measurable quantities (see "line shape", "A_{FB}", "τ polarization", ...).

The weak form factors in (67) are explicitly given by the following set of formulae:

Neutral current vertex:

neutrinos:

$$\begin{aligned} F_V^{Z\nu} &= F_A^{Z\nu} \\ &= \frac{\alpha}{4\pi}\frac{1}{4c_W s_W}\left[\frac{1}{4c_W^2 s_W^2}\Lambda_2(s,M_Z) + \frac{2s_W^2-1}{2s_W^2}\Lambda_2(s,M_W) + \frac{3c_W^2}{s_W^2}\Lambda_3(s,M_W)\right] \end{aligned} \tag{69}$$

charged fermions:

$$\begin{aligned} F_V^{Zf} &= \frac{\alpha}{4\pi}\left[v_f(v_f^2+3a_f^2)\Lambda_2(s,M_Z) + F_L^f\right] \\ F_A^{Zf} &= \frac{\alpha}{4\pi}\left[a_f(3v_f^2+a_f^2)\Lambda_2(s,M_Z) + F_L^f\right] \end{aligned} \tag{70}$$

with

$$\begin{aligned} F_L^l &= \frac{1}{8s_W^3 c_W}\Lambda_2(s,M_W) - \frac{3c_W}{4s_W^3}\Lambda_3(s,M_W) \\ F_L^u &= -\frac{1-\frac{2}{3}s_W^2}{8s_W^3 c_W}\Lambda_2(s,M_W) + \frac{3c_W}{4s_W^3}\Lambda_3(s,M_W) \\ F_L^d &= \frac{1-\frac{4}{3}s_W^2}{8s_W^3 c_W}\Lambda_2(s,M_W) - \frac{3c_W}{4s_W^3}\Lambda_3(s,M_W)\,. \end{aligned}$$

Electromagnetic vertex:

$$\begin{aligned} F_V^{\gamma f} &= \frac{\alpha}{4\pi}\left[Q_f(v_f^2+a_f^2)\Lambda_2(s,M_Z) + G_L^f\right] \\ F_A^{\gamma f} &= \frac{\alpha}{4\pi}\left[Q_f\, 2v_f a_f\,\Lambda_2(s,M_Z) + G_L^f\right] \end{aligned} \tag{71}$$

with

$$\begin{aligned} G_L^l &= -\frac{3}{4s_W^2}\Lambda_3(s,M_W) \\ G_L^u &= -\frac{1}{12s_W^2}\Lambda_2(s,M_W) + \frac{3}{4s_W^2}\Lambda_3(s,M_W) \\ G_L^d &= \frac{1}{6s_W^2}\Lambda_2(s,M_W) - \frac{3}{4s_W^2}\Lambda_3(s,M_W)\,. \end{aligned}$$

The functions Λ_2, Λ_3 have the form [4] ($w = M^2/s$ with $M = M_Z$ or M_W, $s > 0$)

$$\Lambda_2(s,M) = -\frac{7}{2} - 2w - (2w+3)\log(w) \tag{72}$$

[4] Λ_3 only for $s < 4M_W^2$

$$\begin{aligned} &+2(1+w)^2\left[\log(w)\log(\frac{1+w}{w}) - \mathrm{Li}_2(-\frac{1}{w})\right] \\ &-i\pi\left[3+2w-2(w+1)^2\log\left(\frac{1+w}{w}\right)\right] \end{aligned}$$

$$\begin{aligned} \Lambda_3(s,M) &= \frac{5}{6} - \frac{2w}{3} + \frac{2}{3}(2w+1)\sqrt{4w-1}\,\arctan\frac{1}{\sqrt{4w-1}} \\ &-\frac{8}{3}w(w+2)\left(\arctan\frac{1}{\sqrt{4w-1}}\right)^2. \end{aligned}$$

The functions F_L^d and G_L^d cannot be used for b quarks. We do not list the lengthy expressions for F_L^b, G_L^b in this place but refer to the literature [14,40]. They depend explicitly on the top mass and have also a quadratically increasing term $\sim m_t^2/M_Z^2$ if the top is heavy.

The following table 1 contains the values for the leptonic V and A form factors for $s = M_Z^2$ (real parts). Also listed are the Born coupling constants v_e, a_e, eq. (9), in order to exhibit the relative influence of the vertex corrections. s_W^2 is always derived from G_μ and Δr. The Higgs mass is fixed to be $M_H = 100$ GeV; there is, however, no visible change in $F_{V,A}$ if M_H varies from 10 GeV to 1 TeV. The slight top dependence of the form factors is due to the top dependence of s_W^2 entering (70).

Table 1: Leptonic weak form factors ($M_Z = 93$ GeV, $M_H = 100$ GeV)

m_t (GeV)	Re $F_V^{Ze}(M_Z^2)$	Re $F_A^{Ze}(M_Z^2)$	v_e	a_e
50	0.0019	0.0018	-0.0647	-0.6005
100	0.0020	0.0019	-0.0778	-0.6056
150	0.0021	0.0020	-0.0927	-0.6115
200	0.0021	0.0020	-0.1100	-0.6191
230	0.0022	0.0022	-0.1244	-0.6247

The effective coupling constants near the Z peak are (in addition to the contributions from the 2-point functions in 4.2) determined by

$$v_f + \mathrm{Re}\,F_V^{Zf}(M_Z^2) \quad a_f + \mathrm{Re}\,F_A^{Zf}(M_Z^2)\,.$$

They allow an easy estimate of the quantitative effects in various measurable quantities. As examples we demonstrate the size of the vertex contributions in the partial width for $Z \to e^+e^-$ and in the quantity

$$A_e = \frac{2v_e a_e}{v_e^2+a_e^2}\,,$$

which determines the on-resonance asymmetries in case of lepton universality

$$A_{LR} = A_{pol}^\tau = A_e\,, \quad A_{FB}^\mu = \frac{3}{4}(A_e)^2\,,$$

in table 2.

Table 2: Effects of vertex corrections ($M_Z = 93$ GeV, $M_H = 100$ GeV)

m_t (GeV)	$\delta\Gamma/\Gamma(Z \to e^+e^-)$ in %	δA_e	δA_{FB}^u
50	-0.67	-0.0056	-0.00184
100	-0.69	-0.0055	-0.00187
150	-0.72	-0.0053	-0.00188
200	-0.75	-0.0052	-0.00194
230	-0.78	-0.0050	-0.00194

Whereas the vertex corrections for light fermions are practically top independent the form factors for the Zbb vertex increase sizeably for large m_t. This behaviour is shown explicitly in table 3, together with the relative change of the $Z \to b\bar{b}$ partial width due to vertex corrections.

Table 3: Zbb form factors and partial width ($M_Z = 93$ GeV, $M_H = 100$ GeV)

m_t (GeV)	$\mathrm{Re}\, F_V^{Zb}(M_Z^2)$	$\mathrm{Re}\, F_A^{Zb}(M_Z^2)$	$\delta\Gamma/\Gamma(Z \to b\bar{b})$ in %
50	0.0018	0.0017	-0.70
100	0.0019	0.0018	-1.01
150	0.0046	0.0046	-1.81
200	0.0076	0.0076	-2.95
230	0.0099	0.0099	-3.80

In order to give a rough feeling for the vertex corrections, they can be summarized to contribute a correction to the cross section (and width) of $O(1\%)$, in the b case up to 4%.

4.4 The box contributions

The last ingredient in the one-loop corrected amplitudes are the box diagrams with two gauge boson exchange. Again, as done in 4.3, we separate the QED boxes (those where at least one boson is a photon) since they are IR divergent and have to be combined with the interference of initial and final real photon emission at the cross section level in order to give a physical result. These QED corrections are discussed in the context of "A_{FB}" (these proceedings). Here we want to mention only that there are sizeable cancellations between real and virtual photon contributions unless the phase space of the emitted photons is restricted to the soft photon region ($E_\gamma <$ a few GeV).

The genuine weak box diagrams are those with ZZ and WW exchange. They are UV and IR finite (UV divergent only in the unitary gauge). They depend in addition

also on the scattering angle θ resp. the Mandelstam variables

$$t = -\frac{s}{2}(1 - \cos\theta), \quad u = -\frac{s}{2}(1 + \cos\theta)$$

and give the following contributions to the weak amplitude (for $m_f^2 \ll M_W^2$):

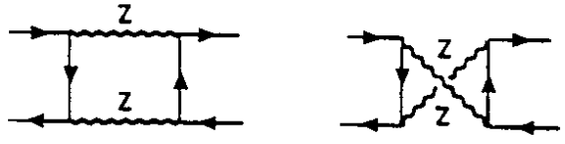

$$= e^2 \frac{J_{NC}^{(e)} \cdot J_{NC}^{(f)}}{s} \cdot \frac{\alpha}{2\pi} [I(s,t,M_Z) - I(s,u,M_Z)] + e^2 \frac{J_{NC}^{(e)5} \cdot J_{NC}^{(f)5}}{s} \cdot \frac{\alpha}{2\pi} [I_5(s,t,M_Z) + I_5(s,u,M_Z)] \tag{73}$$

where

$$\begin{aligned} J_{NC}^{(e)} &= \bar{v}_e \gamma_\mu (v_e^2 + a_e^2 - 2v_e a_e \gamma_5) u_e \\ J_{NC}^{(f)} &= \bar{u}_f \gamma_\mu (v_f^2 + a_f^2 - 2v_f a_f \gamma_5) v_f \\ J_{NC}^{(e)5} &= \bar{v}_e \gamma_\mu \gamma_5 (v_e^2 + a_e^2 - 2v_e a_e \gamma_5) u_e \\ J_{NC}^{(f)5} &= \bar{u}_f \gamma_\mu \gamma_5 (v_f^2 + a_f^2 - 2v_f a_f \gamma_5) v_f \end{aligned} \tag{74}$$

and the functions I, I_5 defined below;

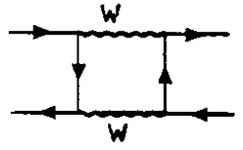

$$= e^2 \frac{J_{CC}^{(e)} \cdot J_{CC}^{(f)}}{s} \cdot \frac{\alpha}{2\pi} [I(s,t,M_W) + I_5(s,t,M_W)] \text{ for } I_3^f = -1/2$$

$$= e^2 \frac{J_{CC}^{(e)} \cdot J_{CC}^{(f)}}{s} \cdot \frac{\alpha}{2\pi} [-I(s,u,M_W) + I_5(s,u,M_W)] \text{ for } I_3^f = +1/2$$

with

$$\begin{aligned} J_{CC}^{(e)} &= \frac{1}{4s_W^2} \bar{v}_e \gamma_\mu (1 - \gamma_5) u_e \\ J_{CC}^{(f)} &= \frac{1}{4s_W^2} \bar{u}_f \gamma_\mu (1 - \gamma_5) v_f \,. \end{aligned} \tag{75}$$

The analytic expressions for I and I_5 read ($f \neq b, t$):

$$
\begin{aligned}
I_5(s,t,M) &= \frac{s}{s+t}\left\{\frac{s+2t+2M^2}{2(s+t)}\left[\mathrm{Li}_2\left(1+\frac{t}{M^2}\right)-\frac{\pi^2}{6}-\log^2\left(-\frac{y_1}{y_2}\right)\right]\right. \qquad (76)\\
&\quad +\frac{1}{2}\,\mathrm{Li}_2\left(-\frac{t}{M^2}\right)+\frac{y_2-y_1}{2s}\,\log\left(-\frac{y_1}{y_2}\right)\\
&\quad \left.+\frac{s+2t-4M^2t/s+2M^2/t-2M^4/s}{2(s+t)(x_2-x_1)}\cdot J(s,t,M)\right\},\\
I(s,t,M) &= I_5(s,t,M)+2\log^2\left(-\frac{y_1}{y_2}\right)+\frac{2}{x_1-x_2}\cdot J(s,t,M),\\
J(s,t,M) &= \mathrm{Li}_2\frac{x_1}{x_1-y_1}+\mathrm{Li}_2\frac{x_1}{x_1-y_2}-\mathrm{Li}_2\frac{x_2}{x_2-y_1}-\mathrm{Li}_2\frac{x_2}{x_2-y_2}
\end{aligned}
$$

with

$$
\begin{aligned}
x_{1,2} &= \frac{1}{2}\left(1\pm\sqrt{1-\frac{4M^2}{s}\left(1+\frac{M^2}{t}\right)}\right),\\
y_{1,2} &= \frac{1}{2}\left(1\pm\sqrt{1-\frac{4M^2}{s}}\right).
\end{aligned}
$$

The more complicated expression for the CC box in $b\bar{b}$ production is not given here (see e.g. ref [40]). Around the Z, the finite fermion mass effects are not important.

Since these box diagrams are non-resonant their contribution near the Z peak is of the order of the $\frac{\alpha}{\pi}$ -corrections to the photon exchange amplitude. This is the reason why their numerical effects in physical quantities on the Z (or not far away) are negligibly small. Their contribution to the differential cross section at $s = M_Z^2$ is smaller than 0.02%. Their influence is slightly bigger at energies which are several GeV below or above M_Z, but still negligible. Figure 7 displays the functions I, I_5 for $s = M_Z^2$, M_Z = 93 GeV.

The smallness of the box contributions to the Z cross section is based on their suppression by the large resonance factor. This should be understood as a warning that box graphs are in general not negligible for processes which are off resonance. As an example we refer to the box contributions to the quantity Δr (the box contributions in muon decay)

$$
(\Delta r)_{box} = -\frac{\alpha}{4\pi}\left(1-\frac{5}{s_W^2}+\frac{5}{2s_W^4}\right)\log c_W^2 = 0.004
$$

which corresponds to a shift $\delta s_W^2 = 0.001$ in the mixing angle.

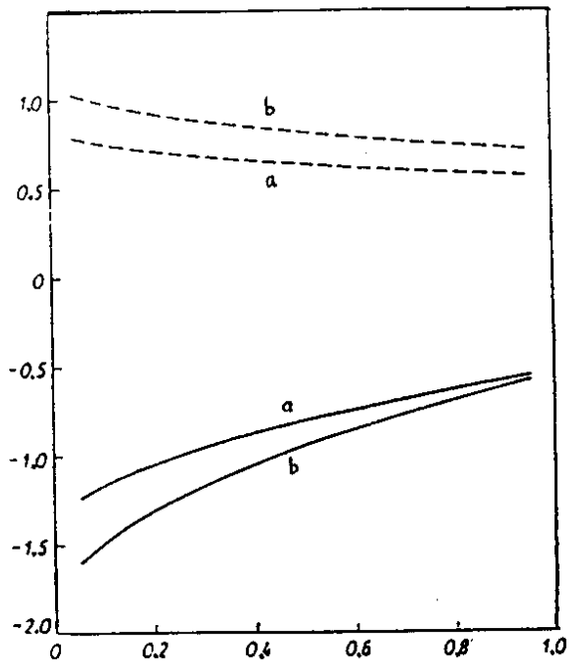

Figure 7:
The functions $I(s,t,M)$ (full) and $I_5(s,t,M)$ (dashed) at $\sqrt{s} = M_Z = 93$ GeV.
a: $M = M_Z$, b: $M = M_W$

4.5 Higher order leading terms and relation to the * scheme

According to our discussion of the 2-point functions in section 4.2, the dressed gauge boson propagators can be expressed with help of 4 renormalized self energy functions

$$\hat{\Sigma}_{WW}(s),\ \hat{\Sigma}_{ZZ}(s),\ \hat{\Sigma}_{\gamma Z}(s),\ \hat{\Sigma}_{\gamma\gamma}(s) \tag{77}$$

which, at present, are calculated to one-loop order. Renormalization affects only their real parts; the imaginary parts, in particular the Z width, can be calculated to $O(\alpha^2)$ with the one-loop renormalized quantities.

As we have also learnt from our discussion in 4.2, dressing the propagators is equivalent to incorporating the real parts via effective coupling constants resp. mixing angle in a Born type amplitude and adding the imaginary parts separately. Thereby the Z width has to be supplemented by the complete $O(\alpha^2)$ contributions for a consistent treatment of the Z propagator around the pole.

The universal character of the propagator corrections can also be expressed in a formally different way by introducing a set of 4 effective parameters

$$e_*(s),\ s^2_*(s),\ G_{\mu *}(s),\ \rho_*(s), \tag{78}$$

as done by Kennedy and Lynn [32]. These running parameters contain the real parts of the self energies; they are arranged in such a way that the amplitude for a 4-fermion process with propagator corrections is obtained from the Born amplitude by the formal replacement

$$(e,\ s^2_W,\ G_\mu,\ \rho) \to (e_*,\ s^2_*,\ G_{\mu *},\ \rho_*), \tag{79}$$

supplemented by the corresponding imaginary parts. When the physical input is taken from the experimental quantities α, G_μ, M_Z, the result for the 4-fermion scattering amplitudes is identical to that of the conventional on-shell scheme with propagator corrections, but without the incorporation of the full $O(\alpha^2)$ contributions to the Z width.

In the following we give the relation between the conventional expressions of section 4.2 and the corresponding ones in terms of the * -parameters:

$$\begin{aligned}
\text{conventional} \quad &\leftrightarrow \quad * \qquad\qquad (80)\\
\frac{e^2}{1+\mathrm{Re}\,\Pi_{\gamma\gamma}(s)} \quad &\leftrightarrow \quad e^2_*(s)\\
\bar{s}^2_W = s^2_W - s_W c_W\,\mathrm{Re}\,\frac{\Pi_{\gamma Z}(s)}{1+\Pi_{\gamma\gamma}(s)} \quad &\leftrightarrow \quad s^2_*(s)\\
\frac{e^2}{s^2_W}\cdot\frac{1}{s-M^2_W+\hat{\Sigma}_{WW}(s)} \quad &\leftrightarrow \quad \frac{e^2_*}{s^2_*}\cdot\frac{1}{s-\frac{c^2_*}{s^2_*}\frac{1}{4\sqrt{2}G_{\mu *}}+i\sqrt{s}\,\Gamma_{*W}(s)}\\
\frac{e^2}{s^2_W c^2_W}\cdot\frac{1}{s-M^2_Z+\Sigma_Z(s)} \quad &\leftrightarrow \quad \frac{e^2_*}{s^2_* c^2_*}\cdot\frac{1}{s-\frac{c^2_*}{s^2_* c^2_*}\frac{1}{4\sqrt{2}G_{\mu *}\rho_*}+i\sqrt{s}\,\Gamma_{*Z}(s)}
\end{aligned}$$

The quantities $\Gamma_{*Z}(s)$, $\Gamma_{*W}(s)$ correspond to the imaginary parts of the Z and W self energies. They can be written in the same way as the tree level widths in the form of (21) but with [32] $e \to e_*$, $s^2_W \to s^2_*$ and $M_{W,Z} \to \sqrt{s}$ due to the variation of the phase space. The relation to the physical Z width (and similar for W) is given by

$$\Gamma_Z = \frac{\Gamma_{*Z}(M^2_Z)+\Delta\Gamma_Z}{1+\kappa_*}$$

where $\Delta\Gamma_Z$ denotes the missing part of the Z width in $O(\alpha^2)$, discussed in (45), [5] and the κ_* is determined by the residue of the Z propagator in (80):

$$s - \frac{e^2_*}{s^2_* c^2_*}\frac{1}{4\sqrt{2}G_{\mu *}\rho_*} = (s-M^2_Z)\cdot(1+\kappa_*).$$

The zero of the l.h.s. corresponds to the physical Z mass.

The * star arrangement as well as the conventional one with resummation of the self energies contain higher order terms which are in general not gauge invariant. The leading terms, however, arise from light and heavy fermions which belong to the gauge invariant subclass of fermion loops, and the resummation yields the reducible higher order terms to all orders. The bosonic loop contributions on the other hand give gauge invariant results only when they are combined with vertex and box diagrams of the same order in a physical matrix element. They have always to be understood as expanded to one-loop order when appearing in formally higher order expressions. In the 't Hooft-Feynman gauge the numerical differences are irrelevant; in the unitary gauge, however, the individual contributions become divergent. Since the resummation of higher order terms is of experimental significance at most for the fermionic leading terms we restrict our following discussion to the large logs in $\Delta\alpha$, eq. (50), associated with the photon vacuum polarization, and the heavy top term $\Delta\bar{\rho}$, defined in (51). From or formulae in section 4.2, in particular from (35) evaluated in the leading terms, we obtain (see also ref [44]):

$$\begin{aligned}
1-\Delta r \;&\approx\; 1-\Delta\alpha+\frac{c^2_W}{s^2_W}\Delta\bar{\rho}-\frac{c^4_W}{s^4_W}\frac{(\Delta\bar{\rho})^2}{1-\Delta\alpha}\\
&=\; (1-\Delta\alpha)\left(1+\frac{c^2_W}{s^2_W}\Delta\rho\right) \qquad\qquad (81)
\end{aligned}$$

where the redefinition

$$\Delta\rho = 3\,\frac{G_\mu m^2_t}{8\pi^2\sqrt{2}}. \tag{82}$$

differs from (51) by a second order term. This allows to find also the leading contribution to the effective mixing angle [6]

$$\bar{s}^2_W\,(=s^2_*) = s^2_W + c^2_W\,\Delta\rho \tag{83}$$

[5] in the definition of Γ_{*Z} in Ref. [32] the QCD correction factor has already been included

[6] note that the s-dependent part is of non-leading structure

which differs from (62) also by a second order term, and to the effective NC coupling strength in (54):

$$\frac{e^2}{4s_W^2c_W^2}\cdot\frac{1}{1+\Pi_Z} \approx \frac{e^2}{4s_W^2c_W^2}\cdot\frac{1}{1-\Delta\alpha+\frac{c_W^2-s_W^2}{s_W^2}\Delta\bar{\rho}-\frac{c_W^4}{s_W^4}\frac{(\Delta\bar{\rho})^2}{1-\Delta\alpha}}$$
$$= \sqrt{2}G_\mu M_Z^2\cdot\frac{1}{1-\Delta\rho}. \qquad (84)$$

On the other hand, the leading terms in the effective coupling of the $*$-scheme

$$\frac{e_*^2}{4s_*^2c_*^2} \approx \frac{e^2}{1-\Delta\alpha}\cdot\frac{1}{4s_W^2c_W^2\left(1+\frac{c_W^2}{s_W^2}\Delta\rho\right)(1-\Delta\rho)} \qquad (85)$$
$$= \sqrt{2}G_\mu M_Z^2\cdot\frac{1}{1-\Delta\rho} \qquad (86)$$

yield the same result as in (84).

Table 4 shows the numerical values for the effective mixing angle $\bar{s}_W^2(M_Z^2)$, as discussed in section 4.2.3, and $s_*^2(M_Z^2)$ obtained from the program EXPOSTAR [45].

Table 4: The effective mixing angle at the Z scale ($M_Z = 93$ GeV, $M_H = 100$ GeV)

m_t (GeV)	$\bar{s}_W^2(M_Z^2)$	$s_*^2(M_Z^2)$
50	0.2212	0.2213
100	0.2202	0.2203
150	0.2189	0.2189
200	0.2171	0.2172
230	0.2159	0.2159

Limitation and improvement:

Since the amplitudes with the $*$ parameters (together with the imaginary parts) correspond to the on-shell amplitudes including the propagator corrections the accuracy is limited by the contributions of the vertex and box corrections which have to be added as well. Thus, everything which has been said about vertex and box corrections in sections 4.3 and 4.4 remains valid also for the amplitudes in the $*$ parametrization.

A second, more general limitation which applies to both formulations comes from the missing 1PI higher order terms. The summation of 1-loop diagrams yields the correct answer only for the leading log's from the light fermions, i.e. all powers

$$\alpha^n \log^n \frac{M_Z^2}{m_f^2}$$

are included in the proper way, according to renormalization group arguments [46]. However, for the heavy top term, already the next order $(\alpha m_t^2/M_Z^2)^2$ contribution does

not have the correct coefficient since the $O(\alpha^2)$ 1PI contribution to $\Delta\rho$ has not yet been implemented. The $O(\alpha^2)$ term can be completed [44] making use of the result in [47] by

$$\Delta\rho \to \Delta\rho + \Delta\rho^{(2)}, \qquad (87)$$

with

$$\Delta\rho^{(2)} = 3\left(\frac{G_\mu m_t^2}{8\pi^2\sqrt{2}}\right)^2 (19 - 2\pi^2). \qquad (88)$$

In figures 8,9 we show the quantities Δr, s_W^2, $\bar{s}_W^2$ as calculated to one-loop order and with the correctly included two-loop leading top contribution.

4.6 Improved Born approximation and effective couplings

For many purposes it may be sufficient to have an improved Born approximation which comprises the leading effects from light fermions and a potentially heavy top quark. Such an improved Born amplitude can easily be derived from the substitution rules given at the end of 4.2, together with the discussion of the leading terms performed in the previous subsection. Here we take into account only the light fermion and the heavy top contributions, together with the structure suggested from the consideration of higher orders in the leading terms (see sections 4.5 and 5.1).

With the matrix elements of the electromagnetic current

$$J_{em}^{(e)} = \bar{v}_e\gamma_\mu u_e, \quad J_{em}^{(f)} = \bar{u}_f\gamma_\mu v_f$$

and $\bar{J}^{(e,f)}$ from (60) the improved Born amplitude for $e^+e^- \to f\bar{f}$ near the Z resonance is given by

$$\overline{M}_{Born} = Q_eQ_f\frac{4\pi\alpha(M_Z^2)}{s}J_{em}^{(e)}\cdot J_{em}^{(f)} \qquad (89)$$
$$+\sqrt{2}G_\mu M_Z^2\,\rho\,\frac{\bar{J}^{(e)}\cdot\bar{J}^{(f)}}{s-M_Z^2+i\frac{s}{M_Z^2}M_Z\Gamma_Z}$$

This expression contains the effective electromagnetic coupling constant which is

$$\alpha(M_Z^2) = \frac{\alpha}{1-\Delta\alpha} = 1.064\,\alpha \qquad (90)$$

for $M_Z = 92$ GeV [48], the normalization of the Z amplitude by the factor

$$\rho = \frac{1}{1-\Delta\rho} \qquad (91)$$

where

$$\Delta\rho = 3\frac{G_\mu m_t^2}{8\pi^2\sqrt{2}}, \qquad (92)$$

and the approximate effective mixing angle

$$\bar{s}_W^2 = \frac{1}{2}\left(1-\sqrt{1-\frac{4A}{\rho M_Z^2(1-\Delta\alpha)}}\right) \qquad (93)$$

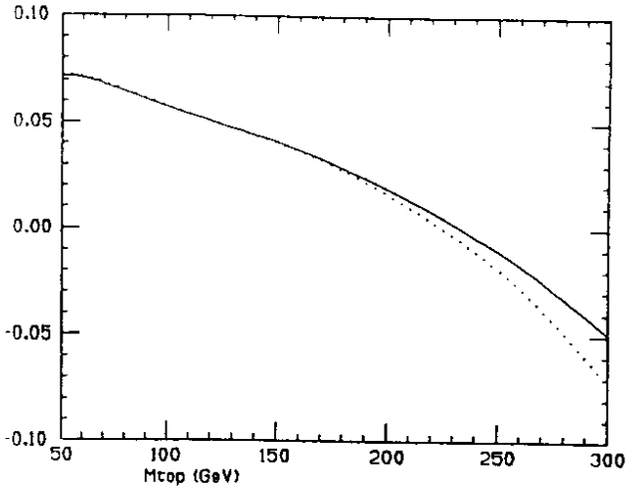

Figure 8:
Δr in $O(\alpha)$ (dotted line) and $O(\alpha^2)$ (solid line).
$M_Z = 91$ GeV, $M_H = 100$ GeV.

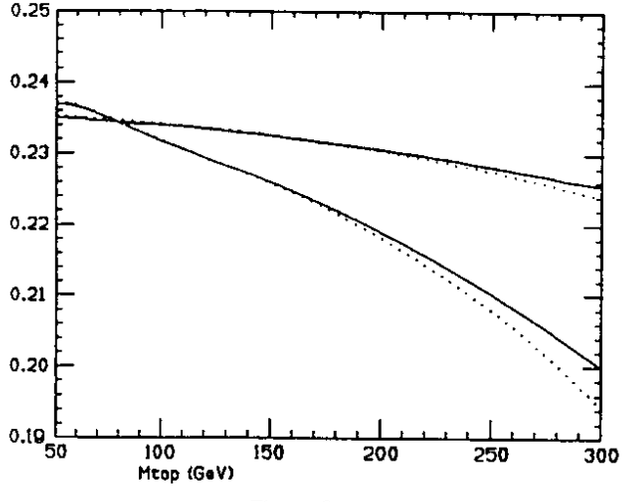

Figure 9:
$\bar{s}^2_W$ (upper curves) and s^2_W (lower curves) in $O(\alpha)$ (dotted) and $O(\alpha^2)$ (full).
$M_Z = 91$ GeV, $M_H = 100$ GeV.

with A given in (17). This expression for $\bar{s}^2_W$ is obtained from the relation

$$\rho\, M_Z^2\, \bar{s}_W^2\, \bar{c}_W^2 \;=\; \frac{A}{1-\Delta\alpha} \tag{94}$$

which follows immediately from [see (18) and (88)]

$$M_Z^2 s_W^2 c_W^2 \;=\; \frac{A}{(1-\Delta\alpha)(1+c_W^2/s_W^2\Delta\rho)}$$

together with (83) and (91).

The width obtained in this approximation is given by

$$\Gamma_Z \;=\; \sum_f \Gamma_Z(Z\to f\bar{f}), \tag{95}$$

with the partial widths (neglecting the finite mass terms)

$$\Gamma_Z(Z\to f\bar{f}) \;=\; N_C^f\,\frac{M_Z}{12\pi}\,\sqrt{2}G_\mu M_Z^2\rho\left[1+(2I_3^f-4Q_f\bar{s}_W^2)^2\right]. \tag{96}$$

The quality of this approximation is displayed in Figures 10 - 14 for various measurable quantities where a comparison is made with the results containing the full electroweak corrections. In the partial widths the above formulae approximate the results within 1%, except for the $b\bar{b}$ partial width. In the asymmetries, the differences can be relatively large, showing the necessity of the complete set of corrections when compared to the experimental accuracy. Note that the improved Born approximation does not contain any information about the Higgs mass.

The unsatisfactory description of the b quark partial width is due to the presence of large top dependent terms in the vertex corrections (see section 4.3). The leading terms $\sim m_t^2$ can easily be incorporated in the set of formulae given above by multiplying the universal quantities ρ and $\bar{s}^2_W$ in (96) with non-universal vertex correction factors ρ_b, κ_b:

$$\begin{aligned}\rho \;&\to\; \rho\left(1-\frac{4}{3}\Delta\rho\right)\equiv\rho_b \\ \bar{s}^2_W \;&\to\; \bar{s}^2_W\left(1+\frac{2}{3}\Delta\rho\right)\equiv\bar{s}^2_W\cdot\kappa_b\,.\end{aligned} \tag{97}$$

In the amplitude (89) with only a single Zbb vertex, ρ has to be replaced by

$$\rho \;\to\; \sqrt{\rho\,\rho_b}\,.$$

The effect of this substitution is displayed in Figure 15 for the b partial width. Now our results approximate the complete ones also within about 1%. Non-leading terms in the vertex corrections, which are numerically more significant than in the self energies, give rise to the deviations from the correct results which are larger than in the case of d-quarks.

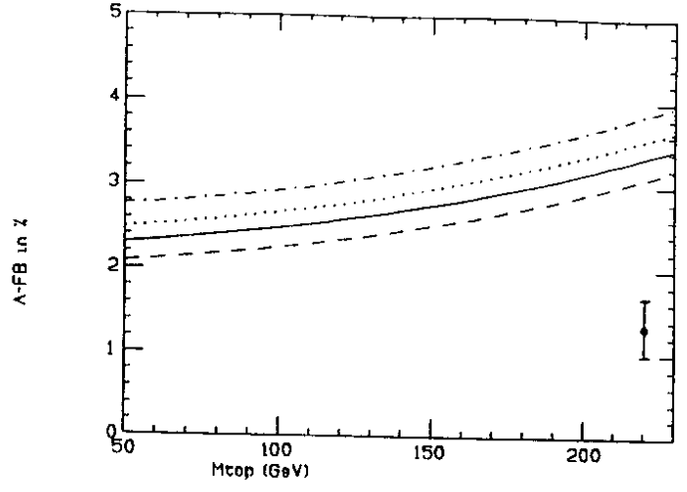

Figure 10:
Forward-backward asymmetry A_{FB} in $e^+e^- \to \mu^+\mu^-$. $M_Z = 92$ GeV.
$M_H = 10$ (···), 100 (—), 1000 GeV (– – –), and improved Born approximation (–·–·–)

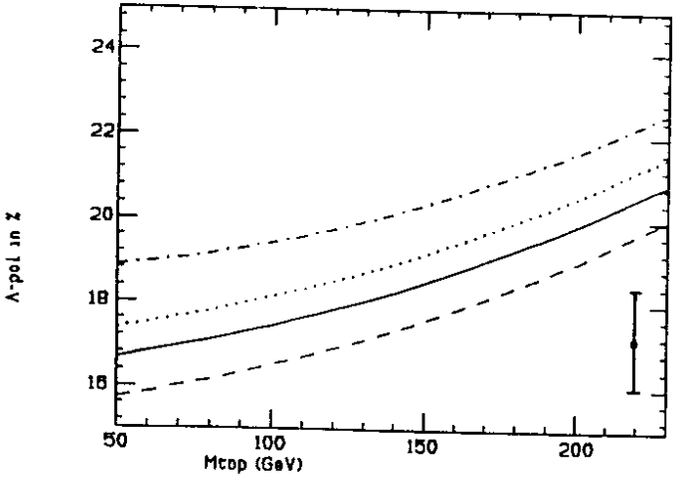

Figure 11:
τ polarization in $e^+e^- \to \tau^+\tau^-$.
Signature as in Figure 10.

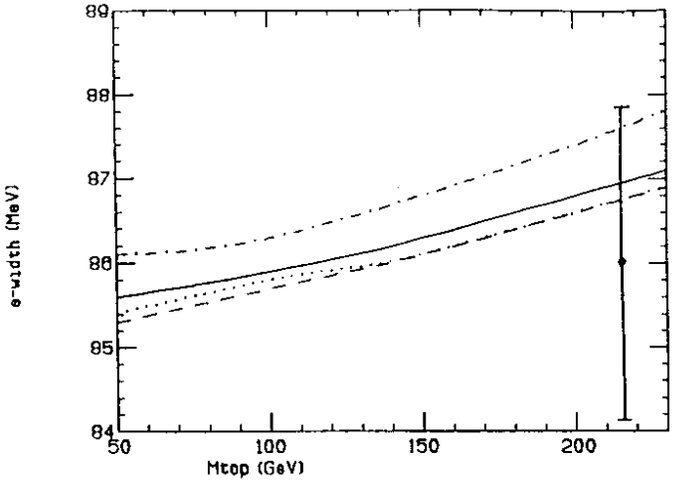

Figure 12:
Electronic partial width (without QED corrections). Signature as in Figure 10.

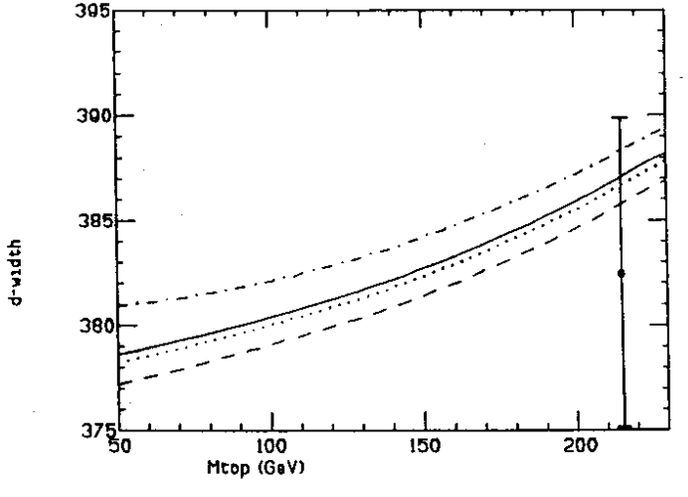

Figure 13:
d quark partial width (without QCD and QED corrections).
Signature as in Figure 10.

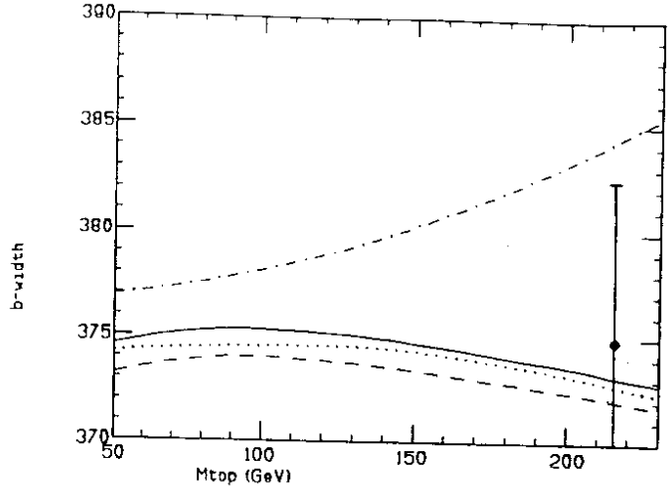

Figure 14:
b quark partial width (without QCD and QED corrections).
Signature as in Figure 10.

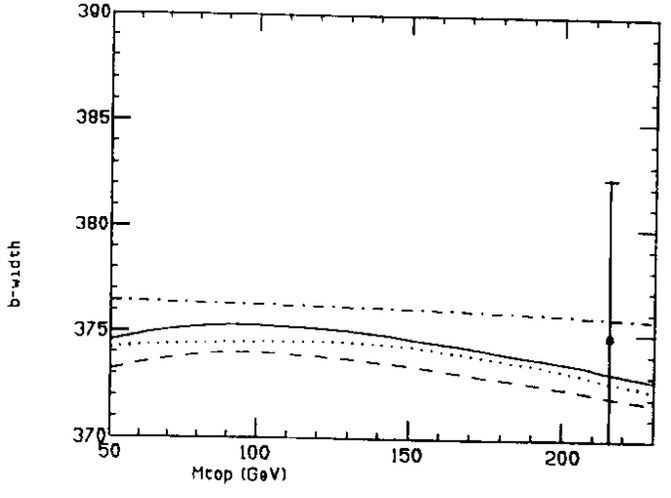

Figure 15:
b quark partial width (without QCD and QED corrections).
Signature as in Figure 10, but now improved Born together with the substitution (97).

Effective couplings at the Z resonance:
The above discussion, which is restricted to the leading light and heavy fermion contributions, provides a simple and gauge invariant calculation of the neutral current couplings in terms of the Z mass. As anticipated at the end of section 4.2, we can introduce a specific normalization ρ_f and weak mixing angle $\sin^2\theta_f$ for each fermion current which summarize all the non-QED corrections at the Z resonance:

$$J^f_{eff} = \left(\sqrt{2}G_\mu M_Z^2 \rho_f\right)^{1/2} \bar{f}\gamma_\mu \left[I_3^f(1-\gamma_5) - 2Q_f \sin^2\theta_f\right] f\,.$$

ρ_f and $\sin^2\theta_f$ are directly measurable from the various on-resonance $f\bar{f}$ asymmetries and Z partial decay widths. They contain the universal self energy discussed in section 4.2, and the non-universal vertex corrections. With exception of $f = b$, these non-universal pieces are small (but not negligible).

5 The $M_W - M_Z$ -interdependence

5.1 The μ decay and Δr

Originally, the μ-lifetime τ_μ has been calculated within the framework of the effective four-point Fermi interaction. If we include the QED corrections we obtain the result given in (12). This formula is used as the defining equation for G_μ in terms of the experimental μ- lifetime. Within the Standard Model, adopting the on-shell scheme with α and the physical particle masses for the input parameters, the Fermi constant coincides with the calculable expression

$$G_\mu = \frac{\pi\alpha}{\sqrt{2}}\frac{1}{M_W^2 s_W^2}\frac{1}{1-\Delta r} \tag{98}$$

where the one-loop correction $1+\Delta r$ to the lowest order result in (13) is usually written in the denominator. In order to get the formal expression for G_μ, and hence for Δr, we have to calculate the μ decay transition amplitude. With the muon (μ) and the electron (e) charged current matrix elements (u and v denote the external spinors)

$$\begin{aligned} J^{(\mu)} &= \bar{u}_{\nu_\mu}\left[\gamma_\mu(1-\gamma_5)\right] u_\mu \\ J^{(e)} &= \bar{u}_e\ \left[\gamma_\mu(1-\gamma_5)\right] v_{\nu_e}. \end{aligned}$$

we find for the μ decay amplitude

$$\begin{aligned} &= \frac{e^2}{2s_W^2}\cdot\left.\frac{J^{(\mu)}\cdot J^{(e)}}{q^2 - M_W^2 + \hat{\Sigma}_{WW}(q^2)}\right|_{q^2\simeq 0} + \cdots \\ &= -\frac{\pi\alpha}{2}\frac{1}{M_W^2 s_W^2}\cdot\frac{J^{(\mu)}\cdot J^{(e)}}{(1-\frac{\hat{\Sigma}_{WW}(0)}{M_W^2})} + \cdots \\ &= -\frac{G_\mu}{\sqrt{2}}\cdot J^{(\mu)}\cdot J^{(e)}. \end{aligned} \tag{99}$$

$\hat{\Sigma}_{WW}$ is the renormalized W self energy from (35), and the dots stand for the vertex and box corrections. Comparing Eqs. (98) and (99) we obtain

$$\Delta r = \frac{\hat{\Sigma}_{WW}(0)}{M_W^2} + \frac{\alpha}{4\pi s_W^2} \cdot (6 + \frac{7 - 4s_W^2}{2s_W^2} \ln c_W^2) \qquad (100)$$

where the last term is the vertex plus box contribution. We should mention that, unlike in the case of the NC processes , in the CC processes there is no natural separation into QED and "weak" contributions. Within the Standard Model the QED corrections to μ decay are not ultraviolet finite. This is in contrast also to the QED corrections for this process if modelled by an effective Fermi interaction, which can be transformed to a NC form via a Fierz transformation. In the Standard Model the only trouble is caused by the photonic box diagram. A term, diagramatically given by

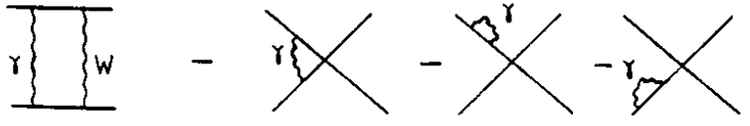

has to be included in the last term of (100). The subtracted term is the one included, by convention, in the QED correction factor of (12).

Assuming that there are no substantial non standard couplings to the external fermions, the vertex plus box contribution is well determined within the Standard Model. Numerically it is smaller than the self-energy corrections by one order of magnitude but it is not negligible. The self-energy contributions are larger and depend on unknown physics, like the top mass, the Higgs mass, on 4th family fermion masses e.t.c. The large and potentially large terms in Δr may be exhibited by writing (to one-loop)

$$\Delta r = \Delta\alpha - \frac{c_W^2}{s_W^2}\Delta\rho + \Delta r_{remainder} \equiv \Delta\alpha + (\Delta r)_W \, . \qquad (101)$$

$\Delta\alpha$ is the photon vacuum polarization contribution (50), large due to the large change in scale from zero momentum (Thomson limit) to the Z-mass scale:

$$\Delta\alpha \; = \; 0.0602 \; + \; \frac{40}{9} \cdot \frac{\alpha}{\pi} \log \frac{M_Z}{92\mathrm{GeV}} \; \pm 0.0009 \qquad (102)$$

yielding the numerical value of $\alpha(M_Z^2)$ given in (90). The numerical value includes the hadronic contribution from the 5 known light quark flavors. It will be discussed in more detail in the next "Δr" contribution. $\Delta r_{remainder}$ summarizes all non-leading corrections, in particular the Higgs contribution, and $(\Delta r)_W$ denotes that part of Δr which is not of electromagnetic origin.

In contrast to $\Delta\alpha$, $\Delta\rho$ is minuscule for light fermions but large for heavy fermions with a light iso-doublet partner [43]

$$\Delta\rho = \frac{\sqrt{2}G_\mu}{16\pi^2}\Sigma_f N_{cf}|m_1^2 - m_2^2|, \qquad (103)$$

where the sum extends over doublets with large mass splittings. For the (t, b) doublet with $m_t^2 \gg m_b^2$ we recover eq. (92). Whereas $\Delta\alpha$ is unchanged by unknown physics, $\Delta\rho$

is sensitive to all kinds of $SU(2)_L$ multiplets which directly couple to the gauge bosons and exhibit large mass-splitting. At one-loop order, there is no quadratic Higgs mass dependence in $\Delta\rho$. This is due to the accidental $SU(2)_R$ symmetry of the Higgs sector in the minimal Standard Model [7], which implies $\rho = 1$ at tree level (Veltman screening) [49]. The leading heavy Higgs contribution to Δr is logarithmic:

$$\Delta r^{Higgs} \simeq \frac{\sqrt{2}G_\mu M_W^2}{16\pi^2}\left\{\frac{11}{3}(\ln\frac{m_H^2}{M_W^2} - \frac{5}{6})\right\} \quad (m_H \gg M_W) \, . \qquad (104)$$

The remainder also contains logarithmic terms which are not negligible numerically. For example, a heavy top would give the contribution

$$\Delta r^{top}_{remainder} = \frac{\sqrt{2}G_\mu M_W^2}{16\pi^2} \cdot 2\left(\frac{c_W^2}{s_W^2} - \frac{1}{3}\right)\ln\frac{m_t^2}{M_W^2} + \cdots \, . \qquad (105)$$

Once Δr is given the W mass can be predicted by using the values α, G_μ, and M_Z from LEP. According to (98) we obtain

$$M_W^2 = \frac{M_Z^2}{2}\left(1 + \sqrt{1 - \frac{4A}{M_Z^2}\frac{1}{1-\Delta r}}\right) \qquad (106)$$

with A defined in (17). This equation expresses the $M_W - M_Z$ interdependence in terms of the observable Δr, which will be directly measured at LEP2, through the relation

$$\Delta r = 1 - \frac{A}{M_W^2}\frac{1}{1 - M_W^2/M_Z^2} \, . \qquad (107)$$

In view of precision experiments the question naturally arises whether the approximate all order resummation, implicit in (98), is accurate enough if we keep for Δr only the one-loop result (101).

5.2 Higher order effects

By using renormalization group arguments [46] one can show that the replacement of the one-loop result

$$1 + \Delta r \; \rightarrow \; \frac{1}{1 - \Delta r}$$

correctly takes into account all orders in $(\Delta\alpha)^n$. Therefore, in a situation where large quantum corrections are only due the renormalization of the electric charge from zero energy up to the vector boson mass scale the expression (106) with Δr from (101) represents a very good approximation to the full result.

This argument may fail in case of a non-negligible $\Delta\rho$ (note the simultaneous enhancement factor c_W^2/s_W^2 in (101)). For example, for $m_t = 230$ GeV one gets

$$\begin{aligned} \left(\frac{c_W^2}{s_W^2}\Delta\rho\right)^2 &= 3.9 \cdot 10^{-3} \\ (\Delta\alpha)^2 &= 3.6 \cdot 10^{-3} \\ (\Delta\alpha) \cdot \frac{c_W^2}{s_W^2}(\Delta\rho) &= 3.7 \cdot 10^{-3} \, . \end{aligned}$$

[7] The $SU(2)_R$ symmetry is only broken by the hypercharge coupling and by the differences in the Yukawa couplings in fermion doublets

The answer for the correct summation of $\Delta\rho$ and $\Delta\rho \cdot \Delta\alpha$ to all orders is given in [44] (see also the discussion in section 4.5):

$$G_\mu = \frac{\pi\alpha}{\sqrt{2}M_W^2 s_W^2} \cdot \frac{1}{1-\Delta\alpha} \cdot \frac{1}{1 + c_W^2/s_W^2\,\Delta\rho_{irr}} . \tag{108}$$

$\Delta\rho_{irr}$ represents the irreducible contribution to the ρ parameter defined from the ratio of neutral current to charged current amplitudes at low energy, i.e.

$$\frac{G_{NC}(0)}{G_{CC}(0)} = \rho = 1 + \Delta\rho_{irr} + (\Delta\rho_{irr})^2 + \cdots = \frac{1}{1-\Delta\rho_{irr}} . \tag{109}$$

In this case, as far as only the leading terms in $\Delta\rho$ are concerned [44], the $M_W - M_Z$ interdependence can be reexpressed in a form which is valid to all orders of perturbation theory:

$$M_W^2 = \frac{\rho M_Z^2}{2}\left(1 + \sqrt{1 - \frac{4A}{\rho M_Z^2}\frac{1}{1-\Delta\alpha}}\right) \tag{110}$$

It is important to note that, differently from the running of α which is not significantly modified by the inclusion of two-loop irreducible contributions, the quantity ρ, as defined in (109), can sizeably differ from the one-loop result. In fact, as shown in [47] and discussed in [44], by including the two-loop irreducible term one finds

$$\Delta\rho_{irr} = N_C^f x_f \left[1 - (2\pi^2 - 19)x_f + \cdots\right] \tag{111}$$

with

$$x_f = \frac{\Delta m_f^2}{8\pi^2}\frac{G_\mu}{\sqrt{2}} \tag{112}$$

and the color factor N_C^f (1 for leptons, 3 for quarks). This means that low energy physics is not sensitive to the direct mass splitting Δm_f^2 in an isodoublet but rather to the effective quantity

$$(\Delta m_f^2)_{eff} = \Delta m_f^2\left[1 - (2\pi^2 - 19)\frac{\Delta m_f^2 G_\mu}{8\pi^2\sqrt{2}} + \cdots\right] . \tag{113}$$

The screening effect, due to the Yukawa coupling with the scalar sector, may become large for a large mass splitting. This phenomenon, if confirmed by a closer inspection of the higher order terms in the perturbative expansion, may have far reaching consequences for our understanding of the Standard Model.

To recapitulate the results of this subsection:

- Eq. (106) with the one-loop Δr from (101) is not an accurate parametrization of the $M_W - M_Z$ interdependence. However, if there are no large quantum corrections besides the leading logarithms associated with the electric charge it is numerically close to the correct result given in (114).

- Eq. (108) together with (109), (111),(112) gives the $M_W - M_Z$ interdependence valid to all orders in the case we restrict the analysis to the interplay betwen the two potentially largest effects in the Standard Model, $\Delta\alpha$ and heavy fermions with a large mass splitting.

- To include correctly the above effects, resummed to all orders, and, at the same time the result of the full one-loop calculation, we have the final expression

$$M_W^2 = \frac{\rho M_Z^2}{2}\left(1 + \sqrt{1 - \frac{4A}{\rho M_Z^2}\left[\frac{1}{1-\Delta\alpha} + \Delta r_{remainder}\right]}\right) \tag{114}$$

where ρ is defined in (109), (111), (112); $\Delta\alpha$ is defined in (50) and numerically given in (102). $\Delta r_{remainder}$, defined in (101), is given explicitly in the Δr study group report.

6 Theoretical Uncertainties

In order to establish in a significant manner possibly small effects from unknown physics we have to know the uncertainties of our theoretical predictions which have to be confronted with the experiments.

The sources of uncertainties in theoretical predictions are the following:

- the experimental errors of the parameters used as an input. With the choice α, G_μ, and M_Z from LEP we can keep these errors as small as possible. The errors from this source are then determined by δM_Z since the errors of α and G_μ are negligibly small. For the mixing angle at resonance

$$\frac{\delta\bar{s}_W^2}{\bar{s}_W^2} = \frac{2\,\bar{c}_W^2}{\bar{c}_W^2 - \bar{s}_W^2}\frac{\delta M_Z}{M_Z} \tag{115}$$

one finds

$$\delta\bar{s}_W^2 \simeq 0.0003 .$$

- the uncertainties from quark loop contributions to the radiative corrections . Here, we have to distinguish two cases: the uncertainties from the light quark contributions to $\Delta\alpha$ and the uncertainties from the heavy quark contributions to $\Delta\rho$. In both cases the uncertainties are due to strong interaction effects, which are not sufficiently under control theoretically. The problems are due to:
(i) the ill-defined QCD parameters. The scale of α_s and the definition and scale of quark masses to be used in the calculation of a particular quantity are quite ambiguous in many cases.
(ii) the bad convergence and/or breakdown of perturbative QCD. In particular at low q^2 and in the resonance regions theoretically poorly known nonperturbative effects are non-negligible.

The theoretical problems with the hadronic contributions of the 5 known light quarks to $\Delta\alpha$ can be circumvented by using the experimental e^+e^--annihilation cross-section $\sigma_{tot}(e^+e^- \to \gamma^* \to hadrons)$ for energies up to 40 GeV, say, and perturbative QCD for the high energy tail. The error [48]

$$\delta(\Delta\alpha) = \pm 0.0009 \tag{116}$$

is dominated by the large experimental errors in the continuum contributions to $\sigma_{tot}(e^+e^- \to \gamma^* \to hadrons)$ below the Υ threshold, and can be improved only by more precise measurements of hadron production in e^+e^--annihilation in the corresponding low energy region. This uncertainty leads to an error of $\delta M_W = 17$ MeV in the W-mass prediction and $\delta \sin^2\theta = 0.0003$ in the prediction of the weak mixing parameters.

The contribution to $\Delta\rho$ from quark doublets with large mass splitting exhibits large QCD corrections of the weak current quark loops. For example, for a heavy top one finds

$$\Delta\rho = \frac{\sqrt{2}G_\mu}{16\pi^2} 3 m_t^2 K_{QCD} + \cdots \tag{117}$$

with

$$K_{QCD} = 1 - \frac{2\pi^2 + 6}{9}\frac{\alpha_s}{\pi} \tag{118}$$

for asymptotically large m_t [50]. Here, m_t is assumed to be the threshold value of the current quark mass. Recently also the numerically important subleading terms have been worked out [51]. Unfortunately, the corrections obtained are not well determined numerically because it remains unclear which scale should be chosen for α_s. Also finite correction to the quark masses have not been taken into account (ambiguity in the definition of m_t).
Again, the problem can be controlled better by using dispersion relations [52,53]. In this approach, the remaining uncertainties in Δr

$$\delta(\Delta r)_{QCD} \simeq \begin{cases} 0.0005 & m_t < 150 GeV \\ 0.0015 \cdot (m_t/250 GeV)^2 & m_t > 150 GeV \end{cases} \tag{119}$$

have been estimated in [53]. In the heavy top region, where $\delta(\Delta r) \simeq c_W^2/s_W^2 \delta(\Delta\rho)$, the error in $\Delta\rho$, which determines the on-resonance couplings, is smaller by a factor of about 1/4 and thus comparable to that of $\Delta\alpha$.

- in case of hadronic final states: For inclusive quantities like $\Gamma(Z \to f\bar{f})$ or $A_{FB}(e^+e^- \to f\bar{f})$ perturbative QCD should be applicable in regions where no hadronic resonances are present. The uncertainties in this case are then determined by the uncertainty in our knowledge of α_s and thus are fairly well under control.

- the uncertainties from omission of higher order effects. After resummation of the leading terms, as discussed in the previous sections, how large are the omitted higher order effects? Since a complete two-loop calculation has not been done, we only can guess how large such effects could be. In the calculation of Δr the difference is given, in the approximation we consider, by using different parameters in the evaluation of $\Delta r_{remainder}$ defined in (101). A supposedly conservative estimate of the error made by omitting the higher order effects has been given in [54,55]

$$\delta(\Delta r)_{higher-order} = \pm 0.001 \tag{120}$$

which can be added quadratically to the hadronic errors.

As a result we can say that the theoretical uncertainties are sufficiently small and thus will not obscure the meaning of precision measurements.

7 Conclusions

In this report we have analyzed the general structure of the higher order electroweak effects relevant for LEP/SLC experiments. We have discussed in detail the on-shell renormalization scheme but also compared our results with those obtained by different authors. The set of formulae includes all vector boson self energy parts, the relevant vertex functions, and box contributions. Some approximate analytical expressions for various quantities (asymmetries, Z decay widths), incorporating the leading terms, have also been presented. Together with the QED corrections, generally dominant but theoretically under control, the discussed weak corrections provide the basic ingredients for precision tests of the Standard Model. If the "minimal" model is correct the calculations of the various observables have to reproduce the experimental results with a choice of the unknown parameters m_t and M_H within a reasonable range (50 GeV $< m_t <$ 200 GeV as favored by present experimental data, 10 GeV$< M_H <$ 1TeV as required for a consistent weak coupling interpretation of the theory). If agreement is found the high precision measurements will considerably restrict the allowed area in the space of the unknown parameters. In this sense the inclusion of radiative corrections is not only a necessity but also a benefit: providing a unique chance to test the quantum structure of the Standard Model and its empirically unknown part.

Acknowledgement
We thank G. Altarelli for his helpful criticism and continous encouragement.

A Vector boson self energies

Here we list the functions $\Sigma_{\gamma\gamma,\gamma Z,ZZ,WW}$ in terms of the on-shell parameters and in dimensional regularization. With the dimension D and the mass scale μ we introduce the symbol for the singular term

$$\Delta_j = \frac{2}{4-D} - \gamma + \log 4\pi - \log\frac{m_j^2}{\mu^2} \tag{121}$$

for a given kind of mass m_j (γ is the Euler constant).

We make use of the abbreviations

$$z = M_Z^2, \quad w = M_W^2, \quad h = M_H^2 .$$

Then the functions read as follows (fermion summation extends also over color in case of quarks):

$$\begin{aligned}
\Sigma_{\gamma\gamma}(s) &= \frac{\alpha}{4\pi}\left\{\frac{4}{3}\sum_f Q_f^2\left[s\Delta_f + (s+2m_f^2)\,F(s,m_f,m_f) - \frac{s}{3}\right]\right. \\
&\quad \left. - 3s\Delta_W - (3s+4w)\,F(s,M_W,M_W)\right\} ,
\end{aligned} \tag{122}$$

$$\begin{aligned}
\Sigma_{\gamma Z}(s) &= \frac{\alpha}{4\pi}\left\{-\frac{4}{3}\sum_f Q_f v_f\left[s\Delta_f + (s+2m_f^2)\,F(s,m_f,m_f) - \frac{s}{3}\right]\right. \\
&\quad + \frac{1}{c_W s_W}\left[\left(3c^2+\frac{1}{6}\right)s + 2w\right]\Delta_W \\
&\quad \left. + \frac{1}{c_W s_W}\left[\left(3c_W^2+\frac{1}{6}\right)s + \left(4c_W^2+\frac{4}{3}\right)w\right]F(s,M_W,M_W) + \frac{s}{9c_W s_W}\right\} ,
\end{aligned}$$

$$\begin{aligned}
\Sigma_{ZZ}(s) &= \frac{\alpha}{4\pi}\left\{\frac{4}{3}\sum_{l=e,\mu,\tau} 2a_l^2 s\left(\Delta_l + \frac{5}{3} - \log(-\frac{s}{m_l^2} - i\varepsilon)\right)\right. \\
&\quad + \frac{4}{3}\sum_{f\neq\nu}\left[(v_f^2+a_f^2)\left(s\Delta_f + (s+2m_f^2)\,F(s,m_f,m_f) - \frac{s}{3}\right)\right. \\
&\quad \left.\left. - \frac{3}{8c_W^2 s_W^2}m_f^2(\Delta_f + F(s,m_f,m_f))\right]\right. \\
&\quad + \left[\left(3 - \frac{19}{6s_W^2} + \frac{1}{6c_W^2}\right)s + \left(4 + \frac{1}{c_W^2} - \frac{1}{s_W^2}\right)M_Z^2\right]\Delta_W \\
&\quad + \left[\left(-c_W^4(40s+80w) + (c_W^2-s_W^2)^2(8w+s) + 12w\right)F(s,M_W,M_W)\right. \\
&\quad + \left(10z - 2h + s + \frac{(h-z)^2}{s}\right)F(s,M_H,M_Z) - 2h\log\frac{h}{w} - 2z\log\frac{z}{w} \\
&\quad \left. +(10z-2h+s)\left(1 - \frac{h+z}{h-z}\log\frac{M_H}{M_Z} - \log\frac{M_H M_Z}{w}\right)\right. \\
&\quad \left.\left. + \frac{2}{3}s\left(1 + (c_W^2-s_W^2)^2 - 4c_W^4\right)\right]\frac{1}{12c_W^2 s_W^2}\right\} ,
\end{aligned}$$

$$\begin{aligned}
\Sigma_{WW}(s) &= \frac{\alpha}{4\pi}\frac{1}{s_W^2}\left\{\frac{1}{3}\sum_{l=e,\mu,\tau}\left[\left(s - \frac{3}{2}m_l^2\right)\Delta_l\right.\right. \\
&\quad \left. + \left(s - \frac{m_l^2}{2} - \frac{m_l^4}{2s}\right)F(s,0,m_l) + \frac{2}{3}s - \frac{m_l^2}{2}\right] \\
&\quad + \frac{1}{3}\sum_{q-doublets}\left[\frac{\Delta_+}{2}\left(s - \frac{5}{2}m_+^2 - \frac{m_-^2}{2}\right) + \frac{\Delta_-}{2}\left(s - \frac{5}{2}m_-^2 - \frac{m_+^2}{2}\right)\right. \\
&\quad + \left(s - \frac{m_+^2+m_-^2}{2} - \frac{(m_+^2-m_-^2)^2}{2s}\right)F(s,m_+,m_-) \\
&\quad \left. + \left(s - \frac{m_+^2+m_-^2}{2}\right)\left(1 - \frac{m_+^2+m_-^2}{m_+^2-m_-^2}\log\frac{m_+}{m_-}\right) - \frac{s}{3}\right] \\
&\quad - \left[\frac{19}{2}s + 3w\left(1 - \frac{s_W^2}{c_W^2}\right)\right]\Delta_W \\
&\quad + \left[s_W^4 z - \frac{c_W^2}{3}\left(7z + 7w + 10s - 2\frac{(z-w)^2}{s}\right)\right. \\
&\quad \left. - \frac{1}{6}\left(w + z - \frac{s}{2} - \frac{(z-w)^2}{2s}\right)\right]F(s,M_Z,M_W) \\
&\quad + \frac{s_W^2}{3}\left(-4w - 10s + \frac{2w^2}{s}\right)F(s,0,M_W) \\
&\quad + \frac{1}{6}\left(5w - h + \frac{s}{2} + \frac{(h-w)^2}{2s}\right)F(s,M_H,M_W) \\
&\quad + \left[\frac{c_W^2}{3}(7z + 7w + 10s - 4(z-w)) - s_W^4 z + \frac{1}{6}\left(2w - \frac{s}{2}\right)\right]\frac{z}{z-w}\log\frac{z}{w} \\
&\quad - \left(\frac{2}{3}w + \frac{s}{12}\right)\frac{h}{h-w}\log\frac{h}{w} \\
&\quad \left. - \frac{c_W^2}{3}\left(7z + 7w + \frac{32}{3}s\right) + s_W^4 z + \frac{1}{6}\left(\frac{5}{3}s + 4w - z - h\right) - \frac{s_W^2}{3}\left(4w + \frac{32}{3}s\right)\right\} .
\end{aligned}$$

The function F can be defined via the integral representation

$$\begin{aligned}
F(s,m_1,m_2) &= -1 + \frac{m_1^2+m_2^2}{m_1^2-m_2^2}\log\frac{m_1}{m_2} \\
&\quad - \int_0^1 dx\,\log\frac{x^2 s - x(s+m_1^2-m_2^2) + m_1^2 - i\varepsilon}{m_1 m_2} .
\end{aligned}$$

F has the property $F(0,m_1,m_2) = 0$. The analytical form can be found in [35,39].

References:

1. S.L. Glashow, Nucl. Phys. B 22 (1961) 579;
   S. Weinberg, Phys. Rev. Lett. 19 (1967) 1264;
   A. Salam, in Proc. of the 8th Nobel Symp., p. 367, ed. N. Svartholm, Almqvist and Wiksell, Stockholm, 1968

2. S.L. Glashow, I. Iliopoulos, L. Maiani, Phys. Rev. D 2 (1970) 1285

3. N. Cabibbo, Phys. Rev. Lett. 10 (1963) 531;
   M. Kobayashi, K. Maskawa, Prog. Theor. Phys. 49 (1973) 652

4. H.Y. Han, Y. Nambu, Phys. Rev. 139 (1965) 1006;
   C. Bouchiat, I. Iliopoulos, Ph. Meyer, Phys. Lett. 138 B (1972) 652

5. G. Arnison et al. (UA1 Collab.), Phys. Lett. 122 B (1983) 103;
   M. Banner et al. (UA2 Collab.), Phys. Lett. 122 B (1983) 476;
   C Rubbia, Nobel Lecture, Rev. Mod. Phys. 57 (1985) 699

6. T. Appelquist, J. Carazzone, Phys. Rev. D 11 (1975) 2856

7. G. 't Hooft, Nucl. Phys. B 33 (1971) 173; ibidem, B 35 (1971) 167

8. E.A. Kuraev, V.S. Fadin, Sov. J. Nucl. Phys. 41 (1985) 446

9. G. Altarelli, G. Martinelli, in: "Physics at LEP", CERN 86-02, eds. J. Ellis and R. Peccei, Vol. 1, p. 47

10. F.A. Berends, G. Burgers, W.L. van Neerven, Phys. Lett. 185 B (1987) 395; Nucl. Phys. B 297 (1988) 429; E: Nucl. Phys. B 304 (1988) 921

11. O. Nicrosini, L. Trentadue, Phys. Lett. 196 B (1987) 551; Z. Phys. C 39 (1988) 479

12. V.S. Fadin, V.A. Khoze, Yad. Fiz. 47 (1988) 1693 (Novosibirsk Preprint 87-157)

13. A.A. Akhundov, D.Yu. Bardin, T. Riemann, Nucl. Phys. B 276 (1986) 1

14. W. Beenakker, W. Hollik, Z. Phys. C 40 (1988) 141

15. F.A. Berends, G. Burgers, W. Hollik, W.L. van Neerven, Phys. Lett. 203 B (1988) 177;
    G. Burgers, in: "Polarization at LEP", CERN 88-06, eds. G. Alexander et al., Vol. 1, p. 121

16. D.Yu. Bardin, A. Leike, T. Riemann, M. Sachwitz, Phys. Lett. 206 B (1988) 539

17. R.E. Behrends, R.J. Finkelstein, A. Sirlin, Phys. Rev. 101 (1956) 866;
    T. Kinoshita, A. Sirlin, Phys. Rev. 113 (1959) 1652

18. Particle Data Book, Phys. Lett. 204 B (1988) 1

19. D.A. Ross, J.C. Taylor, Nucl. Phys. B 51 (1973) 25

20. A. Sirlin, Phys. Rev. D 22 (1980) 971

21. G. Passarino, M. Veltman, Nucl. Phys. B 160 (1979) 151

22. M. Greco, G. Pancheri, Y. Srivastava, Nucl. Phys. B 171 (1980) 118; E: Nucl. Phys. B 197 (1982) 543

23. F.A. Berends, R. Kleiss, S. Jadach, Nucl. Phys. B 202 (1982) 63

24. M. Böhm, W. Hollik, Nucl. Phys. B 204 (1982) 45; Z. Phys. C 23 (1984) 31

25. M. Böhm, W. Hollik, Phys. Lett. 139 B (1984) 213

26. R.W. Brown, R. Decker, E.A. Paschos, Phys. Rev. Lett. 52 (1984) 1192

27. W. Wetzel, Nucl. Phys. B 227 (1983) 1

28. B.W. Lynn, R.G. Stuart, Nucl. Phys. B 253 (1985) 216

29. W. Hollik, Phys. Lett. 152 B (1985) 121

30. B.W. Lynn, M.E. Peskin, R.G. Stuart, in: "Physics at LEP", CERN 86-02, eds. J. Ellis and R. Peccei, Vol. 1, p. 90

31. M. Consoli, A. Sirlin, in: "Physics at LEP", CERN 86-02, eds. J. Ellis and R. Peccei, Vol. 1, p. 63

32. D.C. Kennedy, B.W. Lynn, SLAC-PUB 4039 (1986, revised 1988)

33. D.Yu. Bardin, M.S. Bilenky, G.V. Mitselmakher, T. Riemann, M. Sachwitz, Preprint Berlin-Zeuthen, PHE 89-05 (1989), to appear in Z. Phys. C

34. D.Yu. Bardin, M.S. Bilenky, O.M. Fedorenko, T. Riemann, Dubna Preprint E2-88-324 (1988);

35. M. Böhm, W. Hollik, H. Spiesberger, Z. Phys. C 27 (1985) 523;
    Fortschr. Phys. 34 (1986) 687

36. K.I. Aoki, Z. Hioki, R. Kawabe, M. Konuma, T. Muta, Suppl. Progr. Theor. Phys. 73 (1982) 1

37. J. Fleischer, F. Jegerlehner, Nucl. Phys. B 228 (1983) 1

38. D.Yu. Bardin, P. Ch. Christova, O.M. Fedorenko, Nucl. Phys. B 197 (1980) 1

39. G. Burgers, W. Hollik, in:"Polarization at LEP", CERN 88-06, eds. G. Alexander at al., Vol. 1, p. 136

40. W. Hollik, DESY 88-188 (1988), to appear in Fortschr. Phys.

41. J.D. Bjorken, SLAC-198 (1977);
J. Finjord, Phys. Scripta, 21 (1980) 143;
E. Franco, in: "Physics at LEP", CERN 88-02;
F.A. Berends, R. Kleiss, Nucl. Phys. B 260 (1985) 32

42. G. Altarelli, CERN-TH.5290/89 (1989)

43. M. Veltman, Nucl. Phys. B 123 (1977) 89

44. M. Consoli, W. Hollik, F. Jegerlehner, CERN-TH.5395/89 (1989)

45. D.C. Kennedy, B.W. Lynn, C.J.C. Im, R.G, Stuart, SLAC-PUB-4128 (1988)

46. W.J. Marciano, Phys. Rev. D 20 (1979) 274

47. J.J. van der Bij, F. Hoogeveen, Nucl. Phys. B 283 (1987) 477

48. H. Burkhardt, F. Jegerlehner, G. Penso, C. Verzegnassi, in: "Polarization at LEP", CERN 88-06, eds. G. Alexander et al., Vol. 1, p. 145

49. M. Veltman, Acta Phys. Pol. - B 8 (1977) 475

50. A. Djouadi, C. Verzegnassi, Phys. Lett. 195 B (1987) 265;
A. Djouadi, Nuovo Cim. 100 A (1988) 357

51. D. Yu. Bardin, A.V. Chizhov, Dubna Preprint (1989)

52. F. Jegerlehner, Z. Phys. C 32 (1986) 195

53. B.A. Kniehl, J.H. Kühn, R.G. Stuart, in: "Polarization at LEP", CERN 88-06, eds. G. Alexander et al., Vol. 1, p. 158

54. W. Hollik, H.J. Timme, Z. Phys. C 32 (1986) 125

55. F. Jegerlehner, Z. Phys. C 32 (1986) 425